

Language Model Prompt Selection via Simulation Optimization

Haoting Zhang, Jinghai He, Rhonda Righter, Zeyu Zheng
Department of Industrial Engineering and Operations Research
University of California, Berkeley

With the advancement in generative language models, the selection of prompts has gained significant attention in recent years. A prompt is an instruction or description provided by the user, serving as a guide for the generative language model in content generation. Despite existing methods for prompt selection that are based on human labor, we consider facilitating this selection through simulation optimization, aiming to maximize a pre-defined score for the selected prompt. Specifically, we propose a two-stage framework. In the first stage, we determine a feasible set of prompts in sufficient numbers, where each prompt is represented by a moderate-dimensional vector. In the subsequent stage for evaluation and selection, we construct a surrogate model of the score regarding the moderate-dimensional vectors that represent the prompts. We propose sequentially selecting the prompt for evaluation based on this constructed surrogate model. We prove the consistency of the sequential evaluation procedure in our framework. We also conduct numerical experiments to demonstrate the efficacy of our proposed framework, providing practical instructions for implementation.

Key words: simulation optimization, prompt selection, surrogate model, Bayesian inference

1. Introduction

In recent years, the proliferation of the so-called “language models”, such as the GPT (Generative Pre-trained Transformer) series from [OpenAI \(2023\)](#), has marked a significant advancement in technology and industry ([Chowdhery et al. 2023](#)). Some of most influential language models, such as GPT, are pre-trained so that users can directly use the language models without further training. In this work, when we use the term *language models*, we refer to the language models that are already pre-trained and made available to public, either closed-source or open-source, rather than referring to the training procedures of the language models.

These language models, largely developed by large technological companies, once made publicly available, can serve as an important tool for smaller businesses and non-profit organizations. Studies have shown that small businesses leverage language models for cost-effective customer service solutions, automating responses, and increasing efficiency with limited resources ([De Andrade and Tumelero 2022](#)). Non-profit organizations, as highlighted in recent case studies ([Skiles 2023](#)), have successfully used generative language models to enhance donor engagement and analyze social

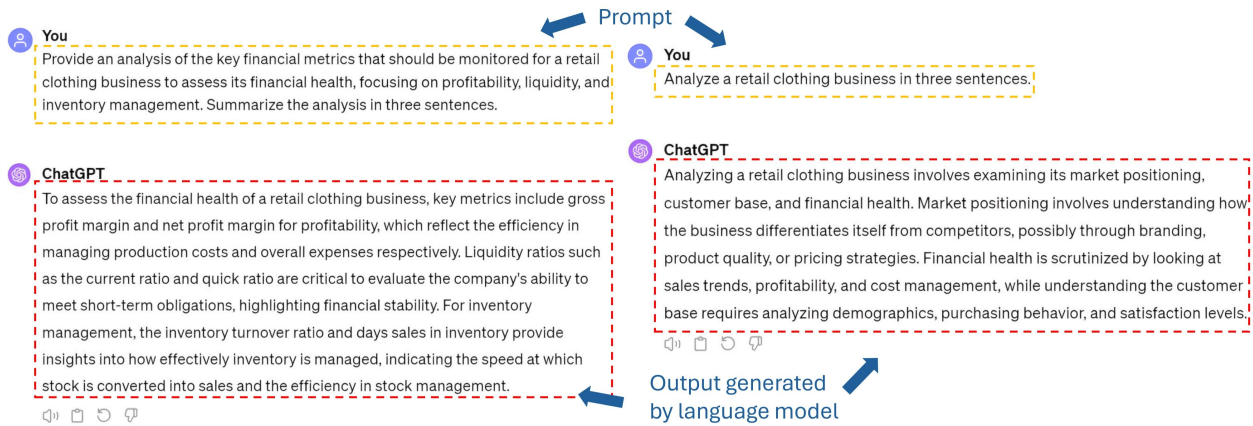


Figure 1 An illustration of different prompts leading to different outputs on the same subject.

impact data, leading to more targeted and effective efforts (Kanter and Fine 2022). These examples illustrate the growing relevance and potential of generative language models for smaller-scale operations, highlighting the need for effective use of language models for these organizations.

One of the cornerstones for effectively leveraging generative language models in smaller enterprises and non-profit organizations emerges in the selection of prompts, which are user-input instructions to guide the generation of outputs from generative language models (Giray 2023). As an example in **Figure 1**, the prompt input by the user describes the requirement for the language model to generate the output. The way a prompt is phrased significantly influences the relevance of the context output by the generative language model. Studies (Horvitz 2023) have shown that well-crafted prompts can even outperform models specifically fine-tuned for applications. Since smaller enterprises and non-profit organizations can suffer from the prohibitive cost of collecting datasets and extensive computational resources of training the generative language model, prompt selection emerges as a promising alternative approach for these organizations with constrained generative language model development capabilities, which underscores the need for research and development in prompt selection.

In most current implementations, the selection and design of the prompts for generative language models heavily rely on human input and subjective guidance (Zamfirescu-Pereira et al. 2023, Hou et al. 2024). These approaches capitalize on the nuanced understanding and creativity inherent in human cognition, allowing for the creation of prompts that tend to be relevant and useful. However, the prompt selection based on human labor also faces room for improvement: (1) Firstly, relying on human labor for prompt design can be a costly process, especially for projects that demand high accuracy and specificity in prompt creation, as it requires extensive time and resources to manually craft and refine prompts. (2) Secondly, manually selecting prompts can limit the scalability and

adaptability of generative language models. As the demand for generative language model services grows, the necessity to rapidly generate and refine prompts for varied tasks becomes more pressing. The manual approach, on the other hand, struggles to keep pace with this demand.

Given the challenges posed by prompt selection based on humans, some more cost-efficient and scalable approaches can be desirable to enhance the effectiveness of prompt selection. In this work, we use the lens of simulation optimization (Hong et al. 2021) to study the prompt selection problem and attempt to provide simulation-optimization based algorithms for prompt selection. In general, simulation optimization handles optimization problems where each sample is costly to obtain (either from an expensive computer simulation of complex systems or from customers/patients in classical or modern clinical trials). Part of the goal of simulation optimization’s algorithm design is to save the sampling costs to achieve a certain requirement of accuracy. We next describe a summary of the prompt selection problem concerned in this work, and how it may be viewed as a simulation optimization problem.

In this work, we facilitate prompt selection as follows: Initially, a prompt is input into the generative language model along with other relevant input contexts, leading to the generation of an output context. Then a score of the prompt is revealed to quantify the effectiveness of the selected prompt. The calculation of the score employs two components: a pre-defined set of baseline output contexts tailored to the task, and a score function that measures the similarity between two contexts. Regarding a specified task, paragraph revision, for example, a baseline set comprises pairs of pre- and post-revision paragraphs. These baseline sets can be collected from a variety of sources including academic publications’ draft and final versions, edit histories of collaborative writing platforms like Wikipedia, or datasets of student essays with teachers’ feedback (Toutanova et al. 2016, Spangher et al. 2022). The score function assesses the similarity between the baseline output and the output generated by the language model (Chandrasekaran and Mago 2021). A higher score indicates greater similarity between the baseline and the generated outputs. The performance of the prompt is then determined by this score. Thus, when the prompt selection is cast as a simulation optimization problem, (1) the decision variable is prompt in text form, (2) the objective to maximize is the score of the prompt, and (3) each prompt evaluation through the language model is regarded as simulating a sample from a stochastic system.

Utilizing simulation optimization methods for prompt selection can encounter challenges. First, the prompt selection does not adopt an explicit feasible set. Indeed, the feasible set is contained in a space that includes any combinations of words and sentences serving as potential prompts. To the best of our knowledge, there have not been simulation optimization methods for such a feasible set. Second, even when the feasible set is restricted to a finite number of prompts, the selection based on existing methods remains challenging. Considering the implicit dependence of the mean score on

the prompt, simulation optimization methods based on certain structures of the objective function, such as convexity and Lipschitz continuity (Eckman et al. 2022), are not feasible. Surrogate models address the lack of transparency in the objective function (Xie et al. 2020, Wang et al. 2023) while existing surrogate models are largely for decision variables represented by vectors instead of the prompts in text form. In addition, there are also simulation optimization methods designed for a finite feasible set without inherent structure, and these methods in general require evaluating each decision variable a sufficient number of times (Hong et al. 2021). However, it is expensive to evaluate each prompt enough times, considering both the computational time to generate contexts and the cost of invoking generative language models.

1.1. Introduction to Our Method and Results

In this work, we propose a framework to facilitate the prompt selection via simulation optimization methods. Our framework is composed of two stages. **1. Search Stage:** This stage determines a feasible set for the prompt selection problem that includes a sufficient but finite number of prompts. The procedure begins by utilizing a text autoencoder, a specialized machine learning model for natural language processing, to transform a few initial example prompts into vectors. These vectors serve as numerical representations of the original text prompts, which are generally high-dimensional. Subsequently, these initial vectors are perturbed, leading to the generation of a larger set of prompts, each uniquely represented by its high-dimensional vector. The next step applies principal component analysis to these vectors to reduce the dimensionality and acquire moderate-dimensional vectors, termed “soft prompts”. The set of soft prompts serves as the feasible set for the prompt selection problem. **2. Evaluation and Selection Stage:** This stage sequentially evaluates the soft prompt decided in the previous search stage. Specifically, we propose constructing a surrogate model of the mean score regarding the moderate-dimensional soft prompt using a Bayesian parametric model. The surrogate model accounts for the uncertainty in the observed scores for prompts, which are assumed to follow a Gaussian distribution. In addition, the surrogate model provides not only the approximated mean score for each soft prompt but also the approximation uncertainty quantification. We then propose an acquisition function based on the surrogate model accounting for both exploitation and exploration. In this way, the sequential evaluation of the prompt is decided by maximizing the acquisition function. When the new observations of scores are collected, the surrogate model and the acquisition function are updated.

Our results are summarized as follows:

1. We consider a prompt selection problem for generative language models to generate the desired outputs, and reformulate it as a simulation optimization problem. We propose a framework that determines the feasible set for a category of simulation optimization problems. In these problems,

the feasible set is not initially provided in an explicit form and therefore requires exploration. Our proposed framework first provides a practical procedure to determine an initial feasible set. When there is sufficient collected data, we also propose a procedure to refine the feasible set construction, which supports further applications and analysis.

2. We propose a surrogate-based simulation optimization algorithm for a finite feasible set, where the surrogate model selection is flexible. We design an acquisition function, for which the trade-off between exploration and exploitation is explicitly addressed by a user-specified hyperparameter. We prove the consistency of the sequential evaluation using a Bayesian parametric model and our proposed acquisition function. Moreover, the optimization of the acquisition function involves approximating its value at each decision variable within the feasible set using simulated samples. Despite the feasible set being finite, this procedure becomes computationally expensive with a large number of decision variables. Therefore, we also consider employing a probabilistic reparameterization method. This method transforms the optimization of the acquisition function from a discrete to a continuous optimization problem. Consequently, the stochastic gradient ascent method is used for optimizing the acquisition function, which is more efficient to implement when the number of decision variables is large. We also prove that the probabilistic reparameterization to speed up the acquisition function optimization does not alter the optimal solution.

3. We conduct numerical experiments to illustrate the efficacy of our proposed framework for prompt selection. Specifically, we demonstrate the superiority of Bayesian neural networks as surrogate models for approximating the mean score of prompts. Additionally, our experiments showcase the efficiency of the probabilistic reparameterization in optimizing the acquisition function, especially when selecting from a large number of prompts. Furthermore, we show that our proposed framework outperforms direct searches in the high-dimensional latent space. Also, the refinement of the feasible set construction improves the mean score of the selected prompts when there are additional evaluations.

Our work may provide the following managerial relevance: First, our framework attempts to offer an efficient method for selecting prompts for generative language models, enhancing their performance without incurring the high costs associated with data collection and extensive computational resources. This approach is particularly beneficial for small businesses and non-profit organizations aiming to leverage generative language models. Secondly, while our focus in this work is on prompt selection, the proposed framework can be adapted to other complex optimization problems across various fields of operational management. For example, drug discovery involves identifying compounds for efficacy and safety within complex chemical spaces, where evaluating each compound combination is costly (Negoescu et al. 2011). Another example is climate modeling, characterized by complex dynamics, where evaluations require intensive computation (Sautner

et al. 2023, Ginglinger and Moreau 2023). These problems typically involve intricate decision variables, implicit objective functions, and costly evaluations. Our framework provides a pathway to alleviate these challenges by converting decision variables into moderate-dimensional vectors and employing surrogate models for efficient selection.

1.2. Literature Review

Our work is relevant to prompt engineering, which is an emerging field within the domain of generative language models. The concept involves crafting effective prompts, which serve as the instructions and task descriptions fed into generative language models to acquire desired outputs. As documented in Giray (2023) and Horvitz (2023), it has been extensively observed that the prompt fed into the generative language model significantly influences the model’s output in terms of relevance, creativity, and accuracy. Pryzant et al. (2023) consider employing gradient descent to optimize the prompt, while these methods are largely restricted to open-source generative language models. In addition, in-context learning algorithms have been utilized to transform a real-valued vector to a human-readable prompt to facilitate the prompt selection (Chen et al. 2023).

In this work, we employ the methodology of simulation to facilitate prompt selection. Simulation experiments have been widely employed to evaluate the performance of complex systems, and application scenarios include but are not limited to finance (Gordy and Juneja 2010, Jiang et al. 2020), queue management (Ibrahim and Whitt 2010, Ibrahim et al. 2012, Ata et al. 2023a,b), etc. In addition to the evaluation of system performance, simulation experiments have also been employed to optimize the system performance with different inputs of the simulation models, which is cast as simulation optimization; see Eckman et al. (2023a,b).

When the feasible set contains a relatively small number of decision variables with no inherent structure defined, the simulation optimization problem is generally cast as ranking and selection (R&S) (Luo et al. 2015, Dong and Zhu 2016, Ni et al. 2017, Hong et al. 2021, Pei et al. 2022, Wu et al. 2022, Hong et al. 2022, Li et al. 2023). In the context of R&S, prominent methods include but are not limited to indifference zone approaches (Fan et al. 2016, 2020, Tsai et al. 2023) and optimal computing budget allocation (He et al. 2007, Fu et al. 2007).

Another stream of literature on simulation optimization focuses on addressing stochastic optimization problems, where the objective function is the expectation of a random function. To estimate this objective function, simulation experiments are conducted to generate samples of the random functions, as discussed in works by (Wu et al. 2018, Lam and Li 2022, Blanchet et al. 2022). In addition to considering the objective function represented by the mean of a random function, simulation optimization also takes into account the risk measures of random functions, such as the quantile and the conditional value at risk, as seen in Deo and Murthy (2023), He et al. (2023).

Additionally, simulation experiments are widely employed to estimate the gradient of the objective function, with detailed discussions found in [Ahamed et al. \(2006\)](#), [Zhu and Dong \(2021\)](#), [Peng et al. \(2022\)](#), [Wang and Hong \(2023\)](#).

Our work benefits from surrogate models in simulation. Surrogate models are statistical models employed to approximate the simulation output, alleviating the expensive execution of simulation models. Owing to this advantage, surrogate models ([Chen et al. 2012](#), [Dong et al. 2018](#), [Wang and Chen 2018](#)) have wide applications in simulation fields, including simulation input uncertainty analysis ([Barton et al. 2014](#), [Xie et al. 2014](#)) and simulation optimization ([L. Salemi et al. 2019](#), [Xie et al. 2020](#), [Semelhago et al. 2021](#), [Hong and Zhang 2021](#), [Wang et al. 2023](#)).

2. Problem Description

In this section, we describe the setting of the prompt selection. We consider a problem context where a user-pre-specified task is given, e.g., aiming to select, from many potential prompts, a good prompt that facilitates paragraph writing refinements. The set of prompts is $\tilde{\mathcal{P}} = \{\mathbf{prom}_1, \mathbf{prom}_2, \dots\}$, where \mathbf{prom}_n denotes a human-readable prompt in text form (e.g., “Revise the following paragraph:”). The prompt and the input context (e.g., the paragraph requiring refinements) are fed into the generative language model and the model generates the output as

$$\hat{\mathbf{y}} = \mathcal{A}(\mathbf{x}, \mathbf{prom}). \quad (1)$$

Here, \mathbf{x} denotes the input context, \mathcal{A} represents the generative language model, and $\hat{\mathbf{y}}$ is the output context generated by the generative language model. We note that, given a fixed pair of input contexts and the prompt $(\mathbf{x}, \mathbf{prom})$, the output contexts $\hat{\mathbf{y}}$ is a random object that can exhibit variability in different trials.

To quantify the performance of a prompt, our framework incorporates two components. Firstly, there is a baseline set, consisting of baseline contexts tailored to the task, providing a standard for comparison. Secondly, a score function is employed to quantitatively assess the quality of the output generated by the generative language model ([Chandrasekaran and Mago 2021](#)). We define the baseline set as $\mathcal{B} = \{(\mathbf{x}_1, \mathbf{y}_1), (\mathbf{x}_2, \mathbf{y}_2), \dots, (\mathbf{x}_M, \mathbf{y}_M)\}$. Each pair $(\mathbf{x}_m, \mathbf{y}_m)$ represents a baseline input-output context. For example, regarding the task of paragraph revision, \mathbf{x}_i denotes the initial paragraph before revision and \mathbf{y}_i denotes the revised paragraph. Such datasets can be collected from academic publications’ draft and final versions, edit histories of collaborative writing platforms like Wikipedia, or datasets of student essays with teachers’ feedback ([Toutanova et al. 2016](#), [Spangher et al. 2022](#)). To evaluate a prompt, say \mathbf{prom}' , we input $(\mathbf{x}_m, \mathbf{prom}')$ into the language model \mathcal{A} , generating the output $\hat{\mathbf{y}}_m$. The score of the prompt \mathbf{prom}' is then calculated using $h(\hat{\mathbf{y}}_m, \mathbf{y}_m)$, where $h(\cdot, \cdot) \in \mathbb{R}$ is the employed score function comparing the generated output $\hat{\mathbf{y}}_m$ with the baseline

\mathbf{y}_m . A detailed description of this score function is provided in the supplements. A higher score implies greater similarity between $\hat{\mathbf{y}}_m$ and \mathbf{y}_m , indicating a ‘better’ performance of the prompt. In this way, given a baseline set \mathcal{B} and a score function $h(\cdot, \cdot)$, the performance of a prompt is evaluated by

$$\hat{v}(\mathbf{prom}) = v(\mathbf{prom}) + \epsilon(\mathbf{prom}).$$

Here, $\hat{v}(\mathbf{prom})$ is the observed score of \mathbf{prom} at each evaluation, $v(\mathbf{prom}) \doteq \mathbb{E}_{(\mathbf{x}_m, \mathbf{y}_m) \sim \mathcal{D}} [h(\mathcal{A}(\mathbf{x}_m, \mathbf{prom}), \mathbf{y}_m)]$ is the mean score of the prompt, and $\epsilon(\mathbf{prom})$ is the uncertainty when observing the score of \mathbf{prom} . We note that the uncertainty $\epsilon(\mathbf{prom})$ comes from two aspects: (1) the random selection of a pair of $(\mathbf{x}_m, \mathbf{y}_m) \in \mathcal{B}$ with equal probabilities, and (2) the phenomenon that language model \mathcal{A} generates different output contexts even when the input context and the prompt are fixed. In this work, we assume the uncertainty ϵ ’s are Gaussian random variables that are independent across different evaluations.

With the mean score of a prompt defined, the selection is formulated as an optimization problem:

$$\mathbf{prom}^* \in \arg \max_{\mathbf{prom} \in \mathcal{P}} v(\mathbf{prom}). \quad (2)$$

That is, we aim to select the prompt that achieves the highest mean score with a fixed baseline set \mathcal{B} and a score function $v(\cdot)$. Considering the implicit dependence of the mean score on the selected prompt, we cast the selection (2) as a *simulation optimization* problem, regarding each evaluation of a prompt as simulating a sample from a stochastic system.

On the other hand, utilizing classical simulation optimization methods for selecting the prompt encounters challenges:

1. **Implicit feasible set:** Regarding the prompt selection problem (2), there is not a specified set of prompts to be selected. The feasible set $\tilde{\mathcal{P}}$ of the optimization problem (2) is defined in a space that contains any potential combination of words and sentences. There is no structural information or prior knowledge of the feasible set $\tilde{\mathcal{P}}$. Existing simulation optimization methods in general consider feasible sets that are either finite or defined within a vector space, which is not feasible for prompt selection.

2. **Non-structural objective function & expensive evaluations:** The prompt selection problem remains challenging even when the feasible set is restricted to be finite. Firstly, given the complex mechanisms of the generative language model, the score as a function at prompts does not exhibit structural properties, such as convexity or Lipschitz continuity. This poses challenges to simulation optimization methods that rely on such structure (Fan and Hu 2018, Eckman et al. 2022). Secondly, while surrogate-based simulation optimization methods are feasible to optimize objective functions lacking explicit structural properties (Quan et al. 2013, Xie et al. 2020, Wang

et al. 2023), these surrogate models in general use vector-represented inputs rather than text-based prompts. Lastly, in cases where the feasible set includes decision variables without inherent structure, the problem can be cast as a ranking and selection (R&S) problem (Hong et al. 2021). On the other hand, most R&S methods require sufficient evaluation of each decision variable. In the context of prompt selection, such extensive evaluation is expensive, considering the computational time and costs associated with engaging the generative language model to generate contexts.

To address these challenges, we propose a framework for prompt selection. The framework is composed of two sequential stages: **1. the search stage** and **2. the sequential evaluation and selection stage**. In the initial search stage, we construct a set of candidate prompts to be evaluated and represent these human-readable prompts with real-valued and moderate-dimensional vectors. We first transform a few prompts in text form to high-dimensional vectors, using the text autoencoder, a specialized machine learning model that numericalizes texts. We then perturb these vectors to attain a larger set of prompts and apply principal component analysis to reduce the dimensionality of the vectors representing prompts. Then, in the evaluation and selection stage, with a finite set of prompts represented by these moderate-dimensional vectors, we propose a sequential evaluation procedure for prompts based on a Bayesian parametric model. Specifically, we construct a surrogate model using the observed scores regarding vector-represented prompts to approximate the mean score of prompts and propose an acquisition function based on the constructed surrogate model. In each round, we select the prompt to be evaluated by maximizing the acquisition function, which accounts for both exploitation (evaluating prompts that have evidence for high scores) and exploration (evaluating prompts with less certainty). When the total budget of prompt evaluation is reached, the prompt that yields the highest mean observed score is selected. We also propose a refinement procedure following the sequential evaluation and selection stage. This involves constructing a surrogate model and a projection mapping from the high-dimensional latent space to a moderate-dimensional subspace. This surrogate model, along with the associated projection mapping, is then used to search for prompts that achieve higher scores than those represented by soft prompts. We present a summary illustration of our framework in **Figure 2**. Section 3 presents the search stage in detail; Section 4 describes the sequential evaluation and selection stage; and the refinement procedure is in Section 5.

3. Search Stage

We now describe the search stage of our proposed prompt selection framework. In this stage, we determine a set of prompts to be evaluated in the next stage and represent these prompts with moderate-dimensional real-valued vectors. Recall that the feasible set $\tilde{\mathcal{P}}$ in the prompt selection problem (2) is in a space that contains any potential combinations of words and sentences in text

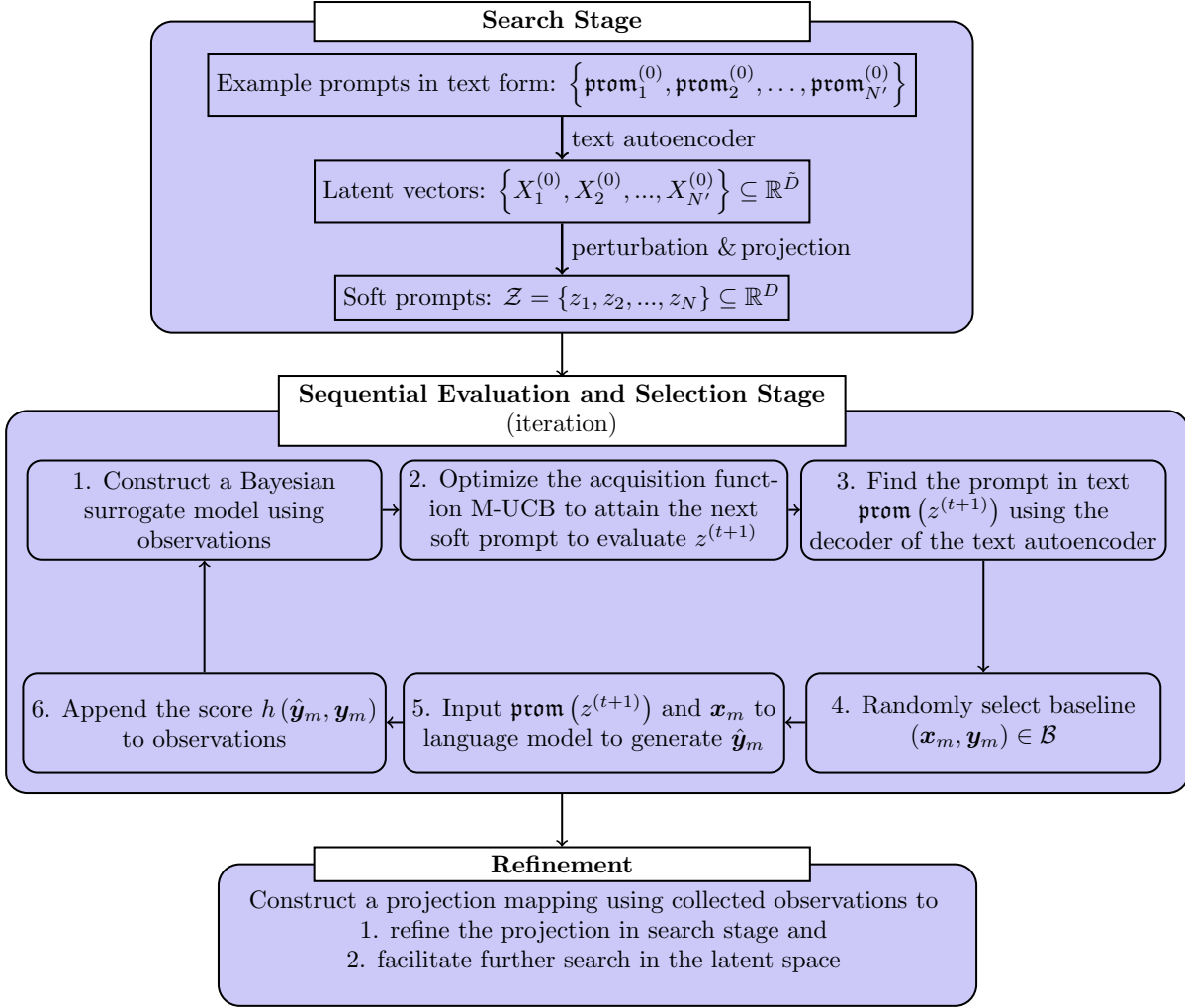


Figure 2 Our framework of prompt selection.

form. In addition to a few example prompts for the specified task, there is no structural information or prior knowledge of deciding a feasible set in the prompt space. To facilitate the selection of the prompt for a specified task, we consider transforming the feasible set $\tilde{\mathcal{P}}$ into a subset in a vector space. This transformation offers two advantages. Firstly, representing prompts as vectors enables their quantitative analysis and manipulation. This numerical representation provides explicit quantification of relationships and patterns among prompts, which may be implicit in their raw text form. Secondly, vector representations of prompts are compatible with existing optimization algorithms, typically tailored for vector-valued decision variables. This compatibility facilitates the use of advanced optimization techniques from fields like machine learning and operations research, thereby enhancing the efficiency and effectiveness of the prompt selection.

Specifically, our procedure begins with a few example prompts that have been recognized as plausible for the specified task. For example, in terms of the paragraph revision task to be accomplished by ChatGPT, these example prompts include: 1. “Please revise the paragraph:”, 2. “Can you revise the paragraph to be more formal and in the third person? Here’s the original paragraph:”, 3. “Could you please revise the paragraph to fix any grammatical errors and enhance its style? The paragraph is as follows:”, etc. These initial example prompts can be attained by previous experiences. Also, some existing work has provided practical procedures to attain these example prompts using in-context learning. Here we refer to [Chen et al. \(2023\)](#).

Instead of selecting from a limited number of these example prompts, it is anticipated that other prompts could lead to higher scores for the revision task. This anticipation is supported by existing prompt engineering procedures accomplished by human efforts; see [Zamfirescu-Pereira et al. \(2023\)](#), [Hou et al. \(2024\)](#). They found that the performance of prompts will be affected by adding descriptions and adverbials, and changing word order, etc. In our framework, the example prompts serve as initial reference points. The scope of the feasible set $\tilde{\mathcal{P}}$ in the prompt selection problem (2), extends beyond these initial examples. On the other hand, actions on the example prompts, such as adding descriptions and adverbials, require human labor and are subjective and expensive in some scenarios. Instead of exploring new prompts directly based on these example prompts, we consider transforming these example prompts to vectors and conducting exploration sampling in the vector space.

Denote the set of the initial example prompts by $\tilde{\mathcal{P}}^{(0)} = \{\mathbf{prom}_1^{(0)}, \mathbf{prom}_2^{(0)}, \dots, \mathbf{prom}_{N'}^{(0)}\}$, where $\mathbf{prom}_n^{(0)}$ is an example prompt for the specified task and N' denotes the number of the example prompts. The procedure in the search stage works as follows. First, these sample prompts are embedded into a vector space $\mathcal{X}^{(0)} \subseteq \tilde{\mathcal{X}} \subseteq \mathbb{R}^{\tilde{D}}$. That is, each example prompt $\mathbf{prom}_n^{(0)}$ is represented by a vector $X_n^{(0)} \in \mathcal{X}^{(0)}$, named *latent vector*. We name $\mathcal{X}^{(0)}$ as the *latent vector set* and denote $\tilde{\mathcal{X}}$ as the *latent space*, which is a subspace of the \tilde{D} -dimensional vector space. In most application scenarios of natural language processing, the latent space is set as $\tilde{\mathcal{X}} = [-1, 1]^{\tilde{D}}$ by default. The procedure of embedding is supported by employing a text autoencoder, and we present the detailed procedure in Section 3.1. Upon completion of embedding, we attain a set of latent vectors $\mathcal{X}^{(0)} = \{X_1^{(0)}, X_2^{(0)}, \dots, X_{N'}^{(0)}\}$, where each $X_n^{(0)} \in \mathbb{R}^{\tilde{D}}$ is a numerical representation of a human-readable example prompt $\mathbf{prom}_n^{(0)}$.

Then, based on these latent vectors, we provide the procedure of constructing a *soft prompt set* in Section 3.2. In this set, each soft prompt is a moderate-dimensional vector and represents a human-readable prompt in text form. This set then serves as the feasible set in the prompt selection problem (2). Specifically, we first extend the latent vector set to

$$\mathcal{X} = \{X_1, X_2, \dots, X_N\} \supseteq \{X_1^{(0)}, X_2^{(0)}, \dots, X_{N'}^{(0)}\} = \mathcal{X}^{(0)}$$

with $N > N'$. Then we apply a dimension reduction algorithm to the latent vector set \mathcal{X} so that each $X_n \in \mathcal{X}$ is transformed to a vector $z_n \in \mathbb{R}^D$ with a moderate dimension D . We denote these moderate-dimensional vectors as soft prompts since each z_n represents a human-readable prompt through the latent vector X_n . Upon completion of the dimension reduction procedure, a soft prompt set $\mathcal{Z} = \{z_1, z_2, \dots, z_N\} \subseteq \mathbb{R}^D$ is attained as a feasible set in preparation for the next evaluation and selection stage in Section 4.

3.1. Prompt Embedding

In this section, we describe the procedure of embedding a human-readable prompt into a real-valued vector. Here we employ fruitful methodologies and models in the area of natural language processing (NLP). Specifically, to attain the vector that represents a human-readable prompt, a text autoencoder model is used in our framework (Li et al. 2015, Kim et al. 2021), formulated as

$$\text{AE}(\text{text}) = \text{Dec}(\text{Enc}(\text{text})) = \text{text}' \quad (3)$$

Here $\text{AE}(\cdot)$ represents the autoencoder model, which is generally composed of two parts: an encoder and a decoder. The encoder model $\text{Enc}(\cdot)$ is a nonlinear mapping that maps a text into a real-valued vector. Then, the decoder takes the vector as the input and outputs another text. Here we focus on the reconstruction of the input text. That is, we aim to train the autoencoder model such that the output text in (3) text' is the same as the input text, i.e., the input text is reconstructed by the text autoencoder model. We postpone the detailed description of the text autoencoder to the supplements.

Note that the human-readable prompts are in text form, which is consistent with the input form of the text autoencoder (3). That is, after appropriate training, the text autoencoder described in (3) can transform each example prompt $\mathbf{prom}_n^{(0)} \in \tilde{\mathcal{P}}^{(0)}$ to a vector $\text{Enc}(\mathbf{prom}_n^{(0)})$ and then transform this vector back to the original prompt $\mathbf{prom}_n^{(0)}$. In this way, we attain 1) a mapping $\text{Dec}(\cdot)$ that transforms a real-valued vector to a text and 2) the vectors $\text{Enc}(\mathbf{prom}_n^{(0)})$'s that represent the initial example prompts. Thus, the latent vector set is $\mathcal{X}^{(0)} = \{X_1^{(0)}, X_2^{(0)}, \dots, X_{N'}^{(0)}\}$, where $X_n^{(0)} = \text{Enc}(\mathbf{prom}_n^{(0)}) \in \mathbb{R}^{\tilde{D}}$, and $\text{Dec}(X_n^{(0)}) = \mathbf{prom}_n^{(0)}$. In addition, for any latent vector $\tilde{X} \notin \mathcal{X}^{(0)}$, the decoder as a mapping transforms it to a human-readable text by $\text{Dec}(\tilde{X})$, though this text might not always be an appropriate prompt for the specified task.

3.2. Soft Prompt Set Construction

We now present the procedure of extending the latent vector set and then projecting these vectors to a subspace with a moderate dimension. These moderate-dimensional vectors then represent the human-readable prompts and are denoted as *soft prompts*.

Recall that we have the set of latent vectors $\mathcal{X}^{(0)} = \{X_1^{(0)}, X_2^{(0)}, \dots, X_{N'}^{(0)}\}$, where each $X_n^{(0)} \in \mathbb{R}^{\tilde{D}}$ represents a human-readable prompt $\text{Dec}(X_n^{(0)})$ for the pre-specified task. Instead of directly exploring the prompt space containing combinations of words and sentences, we search for other potential prompts by sampling new vectors in the latent space. That is, $\forall X^* \in \mathbb{R}^{\tilde{D}}$, the decoder $\text{Dec}(X^*)$ will generate a text output, which might serve as a potential prompt. To decide whether a latent vector X^* is associated with a prompt that will be suitable for the pre-specified task, we compare $\text{Dec}(X^*)$ with a baseline prompt \mathbf{prom}' . The comparison is supported by the score function $v(\cdot, \cdot)$, which quantifies the similarity between two texts. Thus, we retain the latent vector when $v(\text{Dec}(X^*), \mathbf{prom}') \in (r_1, r_2)$, where r_1, r_2 are two user-selected thresholds. The selected thresholds are used to guarantee that the new prompt $\text{Dec}(X^*)$ 1) exhibits sufficient difference from the baseline prompt so that it leads to a different mean score, and 2) maintains certain similarity so that it also works for the task. In this way, we consider sampling new latent vectors based on the initial latent vectors. We first set $\mathcal{X} = \{X_1, X_2, \dots, X_{N'}\}$, where $X_n = X_n^{(0)}$. Then the latent vector set is sequentially extended as follows:

1. Calculate a perturbation matrix $\Sigma_p \in \mathbb{R}^{\tilde{D} \times \tilde{D}}$ based on the current set $\mathcal{X} = \{X_1, X_2, \dots, X_L\}$. In our method, we select the sample covariance matrix for perturbation. That is, $\Sigma_p = \frac{1}{L} \sum_{n=1}^L (X_n - \bar{X})(X_n - \bar{X})^\top$, where $\bar{X} = \frac{1}{L} \sum_{n=1}^L X_n$.
2. Randomly select a latent vector $X_l \in \mathcal{X}$ with probability $p_l = \frac{\exp(-\tilde{n}_l)}{C_L}$, where \tilde{n}_l denotes the number of times X_l has been selected and $C_L = \sum_{n=1}^L \exp(-\tilde{n}_n)$ is a normalizing constant. Then generate from X_l a new latent vector $X' = X_l + V, V \sim \mathcal{N}(\mathbf{0}, \Sigma_p)$.
3. Accept the new latent vector when it 1) remains in the latent space, that is $X' \in \tilde{\mathcal{X}} = [0, 1]^{\tilde{D}}$, and 2) adopts certain similarities with the initial prompt quantified by the score function, that is $v(\text{Dec}(X'), \mathbf{prom}') \in (r_1, r_2)$, where $\mathbf{prom}' = \text{Dec}(X_l)$.
4. If the latent vector X' is not accepted, go back to Step 1. If the latent vector X' is accepted, then append it to the latent vector set \mathcal{X} and go back to Step 1.
5. The procedure terminates when the number of elements in the latent vector set reaches a pre-specified threshold N .

Thus, when the procedure terminates, we attain an extended set of latent vectors $\mathcal{X} = \{X_1, X_2, \dots, X_N\}$. As mentioned in Section 3.1, the dimensionality of the latent vector \tilde{D} is generally high, which imposes challenges to the following evaluation and selection stage, where we construct a surrogate model of the mean value regarding prompt's numerical representations. High-dimensional vectors will increase the sample size required for the surrogate model construction and therefore lead to high costs. Therefore, we conduct a dimensionality reduction procedure for $X_n \in \mathcal{X} \subseteq \mathbb{R}^{\tilde{D}}$. Specifically, we employ the method of principal component analysis (PCA); see [Bro and Smilde \(2014\)](#). The procedure works as follows:

1. Calculate the sample covariance matrix $C = \frac{1}{L} \sum_{n=1}^N (X_n - \bar{X})(X_n - \bar{X})^\top$, where $\bar{X} = \frac{1}{L} \sum_{n=1}^L X_n$. Since the latent vectors are contained in the latent space $\tilde{\mathcal{X}} = [-1, 1]^{\bar{D}}$, here it is not necessary to standardize the latent vectors X_n 's as in a regular procedure of PCA.

2. Decompose the eigenvalue of C by solving the equation $C\mathbf{v} = \lambda\mathbf{v}$ for eigenvalues λ and eigenvectors \mathbf{v} and then sort the eigenvalues and their corresponding eigenvectors in descending order as $\lambda^{(1)} \geq \lambda^{(2)} \geq \dots \geq \lambda^{(\bar{D})}$. This step identifies the directions for the latent vectors that exhibit the most variability by finding the eigenvectors that are associated with the largest values. These directions with the most variability have the potential to be most informative.

3. Let $A^\top = (\mathbf{v}^{(1)}, \dots, \mathbf{v}^{(D)})$ and calculate $z_n = AX_n$ for each $X_n \in \mathcal{X}$. Here D is the selected number of dimensions we would like to retain. In this way, we get the transformed embedding in reduced dimensions and retain the dimensions with the most variability.

This dimensionality reduction procedure also supports the previous procedure for extending the latent vector set. Specifically, the procedure of perturbing existing vectors with the sample covariance matrix has two advantages over traditional methods that use a pre-specified covariance matrix for perturbation. Firstly, it aligns perturbations with PCA, ensuring that the perturbation is fully data-driven and preserves the intrinsic structure and relationships. This contrasts with pre-specified covariance matrices, which lead to a dimension reduction process that reflects the perturbation matrix's structure rather than the structure of the latent space of the prompts. Secondly, this adaptive method allows for the inclusion of new samples that align with the existing prompts' characteristics. In this way, even when high-dimensional vectors are transformed to a moderate dimension, these vectors remain informative, as the dimensionality reduction procedure selectively retains dimensions that reveal important information during the procedure for extending the latent vector set.

Upon completion of dimensionality reduction, we attain a set of z_n 's. We name these moderate-dimensional vectors *soft prompts*. Each soft prompt z_n is associated with the initial latent vector X_n , which further links to a human-readable prompt $\text{Dec}(X_n)$ by the lens of the decoder model in Section 3.1. In this way, the soft prompt set $\mathcal{Z} = \{z_1, z_2, \dots, z_N\}$, which contains finite but sufficient vectors, serves as the feasible set of the prompt selection problem (2) and is provided in preparation for the next evaluation and selection stage.

4. Evaluation and Selection Stage

In this section, we describe the procedure of evaluating and selecting the prompt for a generative language model. The prompts to be evaluated and selected from are represented by moderate-dimensional vectors, termed soft prompts, $z_n \in \mathcal{Z} = \{z_1, z_2, \dots, z_N\} \subseteq \mathbb{R}^D$, where N denotes the number of soft prompts and D denotes the dimension of the vector-valued soft prompt. Each soft

prompt z_n is derived from a latent vector $X_n \in \mathcal{X} \subseteq \mathbb{R}^{\bar{D}}$ by a dimension reduction procedure as in Section 3.2. Thus, we have a one-to-one mapping from z_n to X_n , and the latent vector can be further mapped to a human-readable prompt in text form by applying the encoder $\text{Enc}(X_n)$. In this way, each soft represents a human-readable prompt denoted by $\mathbf{prom}(z_n)$.

Next, we describe the score observation procedure with a selected soft prompt. Our prompt selection procedure involves two components: 1) a baseline set $\mathcal{B} = \{(\mathbf{x}_1, \mathbf{y}_1), (\mathbf{x}_2, \mathbf{y}_2), \dots, (\mathbf{x}_M, \mathbf{y}_M)\}$, where each $(\mathbf{x}_m, \mathbf{y}_m)$ denotes a pair of baseline input-output contexts for comparison; and 2) a score function $h(\cdot, \cdot)$ to quantify the similarities between two contexts. In this way, given a soft prompt z_n , we attain the human-readable prompt $\mathbf{prom}(z_n)$ in text form. We then randomly select a pair of baseline input-output contexts $(\mathbf{x}_m, \mathbf{y}_m)$ from the baseline set \mathcal{B} with equal probabilities. After feeding the human-readable prompt $\mathbf{prom}(z_n)$ and the input context \mathbf{x}_m to the language model, we have the generated output $\hat{\mathbf{y}}_m(z_n) = \mathbf{f}(\mathbf{x}_m, \mathbf{prom}(z_n))$ as in (1), where \mathbf{f} represents the generative language model. By comparing the generated output $\hat{\mathbf{y}}_m(z_n)$ and baseline output context \mathbf{y}_m by the score function, we then observe a score

$$\begin{aligned} \hat{v}_{n,m} &= h(\hat{\mathbf{y}}_m(z_n), \mathbf{y}_m) \\ &= v(\mathbf{prom}(z_n)) + \epsilon_{n,m}. \end{aligned} \tag{4}$$

Here, $v(\mathbf{prom}(z_n)) = \mathbb{E}[\hat{v}_{n,m}]$ is the mean score of the prompt associated with the soft prompt z_n , which serves as the objective function to be maximized. Since the human-readable prompt $\mathbf{prom}(z_n)$ is fully dependent on the soft prompt z_n , we let $v(z_n) \doteq v(\mathbf{prom}(z_n))$ for notational simplicity. In addition, $\epsilon_{n,m} \stackrel{i.i.d.}{\sim} \mathcal{N}(0, \sigma_n^2)$ represents the uncertainty contained in the observed score, which is independent across different selections of z_n and different trials with a fixed z_n . The uncertainty comes from two aspects: 1) the uncertainty from randomly selecting a pair of input-output texts $(\mathbf{x}_m, \mathbf{y}_m)$ from the baseline set \mathcal{B} with equal probabilities, and 2) the inherent uncertainty in the output context $\hat{\mathbf{y}}_m(z_n)$ generation of the language model. That is, even when the prompt $\mathbf{prom}(z_n)$ and the input text \mathbf{x}_m are fixed, the generative language model will generally output different texts, thereby bringing uncertainty in the observed score $\hat{v}_{n,m}$.

In order to find the prompt that achieves the highest mean score $v(z_n)$, we propose a sequential selection procedure that employs a Bayesian parametric model as the surrogate model for the mean score with respect to soft prompts. Specifically, the procedure first selects some soft prompts to observe the scores during the warm-up step (Section 4.1). The observed scores are exploited to construct a surrogate model (Section 4.2.1) and an associated acquisition function (Section 4.2.2). Then, during the sequential evaluation step, the next soft prompt to be evaluated is determined by maximizing the acquisition function. After observing new scores, the surrogate model and the acquisition function are updated and used to guide the selection of the next prompt to be evaluated. The procedure terminates when the budget of evaluating prompts T runs out.

4.1. Warm-up Step

In this section, we describe the warm-up step that observes scores for some soft prompts z_n 's in preparation for the sequential evaluation step. Recall that we have the set of prompts $\mathcal{Z} = \{z_1, z_2, \dots, z_N\}$. In the warm-up stage, we select $N_W (< N)$ soft prompts $z_{W;n} \in \mathcal{Z}$ and for each we observe R scores as in (4). The selection of $z_{W;n}$'s is flexible and user-specified. Here we provide a practical approach. As described in Section 3.2, each soft prompt $z_n \in \mathcal{Z}$ is attained by transforming a latent vector $X_n \in \mathcal{X}$ with a dimension reduction algorithm. Furthermore, this latent vector set \mathcal{X} is expanded by an initial latent vector set $\mathcal{X}^{(0)}$, which contains the latent vectors $X_n^{(0)}$'s that are attained from the initial example prompts $\{\mathbf{prom}_1^{(0)}, \mathbf{prom}_2^{(0)}, \dots, \mathbf{prom}_{N'}^{(0)}\}$. In other words, the soft prompts z_n 's (as well as the human-readable prompts $\mathbf{prom}(z_n)$'s) are attained by perturbing the initial example prompts since the latent vectors are attained by perturbation on the initial latent vectors as the sampling procedure in Section 3.2. Therefore, the soft prompts are generated directly or indirectly from the soft prompts that represent the initial example prompts. Thus, the soft prompts representing the initial example prompts are among the most representative ones, and we therefore select these soft prompts in the warm-up stage to evaluate. That is, we set $\mathcal{Z}_W = \{z_{W;1}, z_{W;2}, \dots, z_{W;N_W}\} \subset \mathcal{Z}$, where $N_W = N'$ and each $z_{W;n}$ is attained by $X_n^{(0)} \in \mathcal{X}^{(0)}$.

After deciding the set \mathcal{Z}_W , we collect $R = 5$ observations for each $z_{W;n} \in \mathcal{Z}_W$. We then approximate the variance of the observed scores $\sigma_n^2 = \text{Var}[\hat{v}_{n,m}]$ by $\hat{\sigma}_n^2 = \frac{1}{R-1} \sum_{r=1}^R (\hat{v}_{n,r} - \bar{v}_n)^2, \forall n \in \{n : z_n \in \mathcal{Z}_W\}$, where $\bar{v}_n = \frac{1}{R} \sum_{r=1}^R \hat{v}_{n,r}$. With the set $\mathcal{D}_W \doteq \{(z_{W;1}, \hat{\sigma}_{W;1}^2), \dots, (z_{W;N_W}, \hat{\sigma}_{W;N_W}^2)\}$, we construct a predictive model $g^*(z_n) \in \mathbb{R}, z_n \in \mathcal{Z}$ by $g^* \in \arg \min_{g \in \mathcal{G}} \sum_{z_n \in \mathcal{Z}_W} (g(z_n) - \hat{\sigma}_n^2)^2$, where \mathcal{G} denotes a class of predictive models (e.g., a linear regression model with unknown parameters) and the selection of the predictive model is flexible and user-specified. In our experiments, we use the kriging method as suggested by Ankenman et al. (2010). After the predictive model g^* is attained, we then approximate σ_n^2 for $\forall z_n \in \mathcal{Z}$ by $g^*(z_n)$. In our work, we treat the variance σ_n^2 as a nuisance parameter, and the difference between the approximated variances $g^*(z_n)$'s and the ground-truth variances σ_n^2 's will be ignored. These approximated variances will be incorporated into the surrogate model in the sequential evaluation step, which resembles classical surrogate models construction (Ankenman et al. 2010, Chen et al. 2012, 2013).

4.2. Sequential Evaluation Step

In this section, we describe the sequential evaluation step, which consists of two actions:

1. **Approximation of Mean Score:** We approximate the mean score of each soft prompt, from historical data of observed scores by constituting a Bayesian parametric model. This model also provides the explicit uncertainty quantification of the mean score approximation.

2. Optimization of Acquisition Function: Once the surrogate model is constructed, the next step involves optimizing an acquisition function that accounts for both the approximated mean scores of each soft prompt and the approximation uncertainty. The next soft prompt to be evaluated is decided by maximizing the acquisition function.

4.2.1. Bayesian Parametric Surrogate Model We assume that the mean performance v with respect to the soft prompt z is represented by a parametric model $v(z) = \mathbf{f}(z; \mathbf{W})$, where the form of the model $\mathbf{f}(\cdot; \cdot)$ is known and $\mathbf{W} \in \mathbb{R}^p$ is an unknown parameter. In this work, the selection of the parametric model is flexible, and we propose a procedure to sequentially select the soft prompt z_n to evaluate using Bayesian inference. Specifically, we regard the unknown parameter as a random vector with prior distribution $\pi(\mathbf{W})$. Suppose we have evaluated the prompts for t rounds (including the observations in the warm-up step), and have collected the observed scores $\mathcal{S}_t \doteq \{(z^{(1)}, \hat{v}^{(1)}), \dots, (z^{(t)}, \hat{v}^{(t)})\}$. Here $z^{(\tau)} \in \mathcal{Z} = \{z_1, z_2, \dots, z_n\}$ denotes the selected soft prompt in the τ -th round, and $\hat{v}^{(\tau)}$ is the observed score associated with $z^{(\tau)}$ as in (4). We note that an equivalent representation of the dataset is $\mathcal{S}_t = \{(z_n, \hat{v}_{n,m})\}$ for $m \in \{1, 2, \dots, r_n(t)\}$ and $n \in \{1, 2, \dots, N\}$. Here $\hat{v}_{n,m}$ denotes the m -th observed score for soft prompt z_n as in (4), and $r_n(t)$ denotes the number of evaluations at z_n up to time t . That is, $\sum_{n=1}^N r_n(t) = t$. Conditional on the dataset \mathcal{S}_t , the posterior distribution of \mathbf{W} is updated by

$$p(\mathbf{W} | \mathcal{S}_t) = \frac{p(\mathcal{S}_t | \mathbf{W}) \pi(\mathbf{W})}{p(\mathcal{S}_t)} \propto p(\mathcal{S}_t | \mathbf{W}) \pi(\mathbf{W}), \quad (5)$$

where

$$p(\mathcal{S}_t | \mathbf{W}) = \prod_{n=1}^N \prod_{m=1}^{r_n(t)} \frac{1}{\sqrt{2\pi\sigma_n^2}} \exp\left(-\frac{(\hat{v}_{n,m} - \mathbf{f}(z_n; \mathbf{W}))^2}{2\sigma_n^2}\right)$$

is the likelihood of the observed scores. In this way, inference for the mean score function is based on $\mathbf{f}(z_n; \widehat{\mathbf{W}})$, $\widehat{\mathbf{W}} \sim p(\mathbf{W} | \mathcal{S}_t)$. For parametric models in which the exact posterior is intractable, Markov Chain Monte Carlo (MCMC) methods (Asmussen and Glynn 2007) or variational inference (VI) (Blei et al. 2017) can be employed to approximate and generate samples from the posterior distribution. We postpone the sampling methods of the posterior distribution to the supplements.

The reason for selecting a Bayesian parametric model for approximating the mean score function is two-fold. 1. Why do we use a surrogate model? Although simulation optimization methods for the finite feasible set have been extensively explored in existing literature, these algorithms in general require either 1) a specific known structure of the objective function (convexity, Lipschitz continuity, etc.) or 2) evaluating each decision variable a sufficient number of times. In the context of the prompt selection, it is not guaranteed that the mean score of the prompts has such a structure. Also, it is also expensive to evaluate each prompt for enough times, considering both the computational time to generate output contexts and the cost of invoking proprietary generative

language models. On the other hand, each prompt to be evaluated is represented by a vector-valued soft prompt z_n . The mean score of the soft prompt has an implicit dependence on the vector z_n , and we use a surrogate model to approximate the dependence. Thus, for a prompt that has never been evaluated, we also have inference based on the surrogate model, which is constructed with observations associated with other prompts. 2. Why do we employ Bayesian inference? In order to sequentially evaluate the prompt in an efficient manner, the trade-off between exploitation and exploration must be addressed appropriately. That is, we are supposed to evaluate the prompt that has the evidence to achieve a high score (exploitation) while evaluating the prompt that has more uncertainty to achieve a high score (exploration). Thus, in addition to the approximated value of the mean score $v(\cdot)$, the uncertainty of the approximation is also required. Bayesian inference provides an effective strategy to quantify the approximation uncertainty, which is used to address the exploitation-exploration trade-off.

We now provide two examples of the parametric model that can be employed in our approach.

EXAMPLE 1 (GAUSSIAN PROCESS). The Gaussian process (GP) has been widely employed in extensive applications including simulation input uncertainty analysis (Xie et al. 2014, Barton et al. 2014) and simulation optimization (Quan et al. 2013, Wang et al. 2023). Specifically, the GP-based method assumes that $\mathbf{f}(z) \sim \mathcal{GP}(0, \mathbf{K}(z, z'))$, where $\mathbf{K}(z, z')$ is a pre-specified kernel function. The kernel function quantifies the similarity of the surrogate model f between different inputs z 's. A common selection is the radial basis function (RBF) kernel $\mathbf{K}_{\text{RBF}}(z, z') = \exp\left\{-\frac{\|z-z'\|^2}{\sigma^2}\right\}$, where $\|\cdot\|$ denotes the Euclidean norm of a vector and σ^2 is a user-specified hyperparameter. Given the observed points, inference for the function value f at an arbitrary point \tilde{z} is based on the conditional distribution of a multivariate normal distribution. That is, $\mathbf{f}(\tilde{z}) \mid \tilde{\mathbf{S}}_t \sim \mathcal{N}(\mu_{GP;t}(\tilde{z}), \sigma_{GP;t}^2(\tilde{z}))$. Here, $\tilde{\mathbf{S}}_t = \{(z^{(1)}, y^{(1)}), \dots, (z^{(t)}, y^{(t)})\}$ denotes the pairs of inputs and observations up to time t , where $y^{(\tau)} = \mathbf{f}(z^{(\tau)}) + \epsilon^{(\tau)}$ denotes the noisy observation, and $\epsilon^{(\tau)} \stackrel{i.i.d.}{\sim} \mathcal{N}(0, \sigma^2)$ denotes the noise. The conditional mean and variance adopt explicit expressions

$$\mu_{GP;t}(\tilde{z}) = \mathbf{K}_t(\tilde{z})^\top \left(\tilde{\mathbf{K}}_t + \sigma^2 \mathbf{I}_t\right)^{-1} \tilde{\mathbf{y}}_t, \quad \sigma_{GP;t}^2(\tilde{z}) = \mathbf{K}(\tilde{z}, \tilde{z}) - \mathbf{K}_t(\tilde{z})^\top \left(\tilde{\mathbf{K}}_t + \sigma^2 \mathbf{I}_t\right)^{-1} \mathbf{K}_t(\tilde{z}), \quad (6)$$

where $\tilde{\mathbf{y}}_t = (y^{(1)}, \dots, y^{(t)})^\top \in \mathbb{R}^t$ is the vector of observations; $\tilde{\mathbf{K}}_t \in \mathbb{R}^{t \times t}$ is the kernel matrix with (τ, τ') -th entry $\mathbf{K}(z^{(\tau)}, z^{(\tau')})$; and $\mathbf{K}_t(\tilde{z}) = (\mathbf{K}(\tilde{z}, z^{(1)}), \mathbf{K}(\tilde{z}, z^{(2)}), \dots, \mathbf{K}(\tilde{z}, z^{(t)}))^\top \in \mathbb{R}^t$ is the vector of kernel function values between \tilde{z} and $\{z^{(\tau)}\}_{\tau=1}^t$.

The GP model is generally regarded as a Bayesian nonparametric model. However, when the selected kernel function has a finite rank, that is $\mathbf{K}(z, z') = \phi(z)^\top \phi(z')$ for $\phi(z) \in \mathbb{R}^p$, the GP model has an alternative parametric representation $\mathbf{f}(z; \mathbf{W}) = \phi(z)^\top \mathbf{W}$. Here, $\mathbf{W} \in \mathbb{R}^p$ denotes the unknown parameter with the prior distribution $\pi(\mathbf{W}) \stackrel{D}{=} \mathcal{N}(\mathbf{0}_p, \mathbf{I}_p)$, and the posterior distribution of the unknown parameters is $p(\mathbf{W} \mid \tilde{\mathbf{S}}_t) \stackrel{D}{=} \mathcal{N}\left(\left(\Phi_t^\top \Phi_t + \sigma^2 \mathbf{I}_t\right)^{-1} \Phi_t^\top \tilde{\mathbf{y}}_t, \sigma^2 \left(\Phi_t^\top \Phi_t + \sigma^2 \mathbf{I}_t\right)^{-1}\right)$,

where $\Phi_t = [\phi(z^{(1)}), \dots, \phi(z^{(t)})]^\top \in \mathbb{R}^{t \times m}$. In this way, inference for $\mathbf{f}(\tilde{z}; \widehat{\mathbf{W}}) = \phi(\tilde{z})^\top \widehat{\mathbf{W}}$ with the posterior distribution $\widehat{\mathbf{W}} \sim p(\mathbf{W} | \tilde{\mathcal{S}}_t)$ matches the results in (6). That is, GP is equivalent to a Bayesian parametric model, parametrized by \mathbf{W} when the kernel function has a finite rank.

As documented in Shen et al. (2018), Ding and Zhang (2022), the performance of GP-based algorithms depends heavily on the appropriate selection of the kernel function $\mathbf{K}(z, z')$. In some applications when the unknown function to be approximated has highly non-structural dependence on the inputs, it is challenging to pre-specify the employed kernel function. Furthermore, because of calculating the inverse matrix, GP-based algorithms suffer from computational complexities of the cubic order of the observed data. Thus, existing work also considers incorporating Bayesian inference with deep learning models to enhance the model’s flexibility and inference accuracy. Next we consider the neural network (Peng et al. 2022, Wang and Hong 2023) as an example, where the weight parameters of the neural network are regarded as random and updated by data as in (5).

EXAMPLE 2 (BAYESIAN NEURAL NETWORK). Neural networks are computing systems that are used to approximate unknown mappings. A neural network is composed of connected layers of nodes, which are denoted as *neurons*. The layers of a neural network include the input layer, the output layer, and the hidden layers that connect the input layer and the output layer. For each pair of adjacent layers, the input of the latter layer is the output of the former layer. The connection between the neurons of adjacent layers is represented by the linear functions, while the *activation function* in each layer imposes non-linearity to the neural network. To be more specific, let $\mathbf{f}(z; \mathbf{W})$ be the neural network with L layers of hidden layers. The innermost layer (the input layer) is represented as the initial layer, and suppose the l -th layer contains m_l neurons. Thus, $m_0 = d^{\text{in}}$ and $m_{L+1} = d^{\text{out}}$, consistent with the dimensions of the inputs and outputs of the mapping to be approximated. In this way, the neural network $\mathbf{f}(z; \mathbf{W})$ is represented as

$$\mathbf{f}(z; \mathbf{W}) = W_L \cdot \varphi(W_{L-1} \cdots \varphi(W_0 z + b_0) \cdots + b_{L-1}) + b_L.$$

Here, W_l is the $m_{l+1} \times m_l$ weight matrix, and b_l is the m_{l+1} -dimensional intercept. All these weight matrices and intercepts compose the weight parameters \mathbf{W} of a neural network. The activation function $\varphi(\cdot)$ is defined on each entry (neuron) respectively and imposes non-linearity to the neural network. Common selections of activation functions include the rectified linear unit (ReLU) function and the tanh function. When the weight parameters are regarded as random variables and adopt a prior distribution, the neural network $\mathbf{f}(z; \mathbf{W})$ is known as a *Bayesian neural network*.

Other models including Bayesian linear regression models (Minka 2000), Bayesian hierarchical models (Rouder and Lu 2005) and variational autoencoders (VAE) (Kingma et al. 2019) can also be employed to approximate the mean score function $v(\cdot)$. The selection of the surrogate model

is flexible and depends on the complexity of the problem and the sample size of the observations. For example, when there are not sufficient observations, the parametric model with few parameters and a relatively explicit form (e.g., Bayesian linear regression model) is preferred. On the other hand, when a large number of observations have been acquired and the mean score is highly non-structural with soft prompts, deep learning models can achieve better performance. With the specified Bayesian parametric model in hand, we next describe the *acquisition function*, which is used to guide the selection of the soft prompt to be evaluated in the next round.

4.2.2. Acquisition Function & Optimization In this section, we present the acquisition function in the sequential evaluation step, which is used to guide the selection of the next soft prompt $z^{(t+1)}$ to be evaluated. Based on the surrogate model in each round $\mathbf{f}(z; \widehat{\mathbf{W}})$, $\widehat{\mathbf{W}} \sim p(\mathbf{W} | \mathcal{S}_t)$, we propose an acquisition function named *Modified Upper Confidence Bound (M-UCB)*, defined on $z_n \in \mathcal{Z} = \{z_1, z_2, \dots, z_N\}$,

$$\alpha_t(z_n) = \mu_t(z_n) + \beta_t(\sigma_t(z_n) + \gamma(r_n(t))). \quad (7)$$

Here $\mu_t(z_n) = \mathbb{E}[\mathbf{f}(z_n; \widehat{\mathbf{W}}) | \mathcal{S}_t]$ and $\sigma_t(z_n) = \left\{ \text{Var}[\mathbf{f}(z_n; \widehat{\mathbf{W}}) | \mathcal{S}_t] \right\}^{1/2}$ are the posterior mean and standard deviation of the surrogate model at z_n , and $r_n(t)$ denotes the number of evaluations at z_n up to time t . In addition, $\{\beta_\tau \in \mathbb{R}\}_{\tau=1,2,\dots,t}$ is a user-selected non-decreasing sequence, and $\gamma(\cdot) \in \mathbb{R}$ is a pre-specified decreasing function defined on $\mathbb{N} = \{0, 1, 2, \dots\}$ satisfying $\lim_{n \rightarrow \infty} \gamma(n) = 0$. The soft prompt to be evaluated in the next round is selected via maximizing the acquisition function. That is, $z^{(t+1)} \in \arg \max_{z_n \in \mathcal{Z}} \alpha_t(z_n)$, where $z^{(t+1)}$ denotes the soft prompt to be evaluated in the next round. Then, after observing the score $\widehat{v}^{(t+1)}$, the surrogate model is updated via updating the posterior distribution (5) with $\mathcal{S}_{t+1} = \{(z^{(t+1)}, \widehat{v}^{(t+1)})\} \cup \mathcal{S}_t$. The sequential selection procedure iterates until the number of rounds t meets the total budget T . We summarize the procedure of the entire evaluation and selection stage in **Algorithm 1**.

The acquisition function M-UCB explicitly balances the exploitation-exploration trade-off via adapting the hyperparameter β_t . Specifically, the posterior mean represents the model’s current approximation of the objective function’s value at a given point, guiding the exploitation of known high-performing areas. The exploration is led by both the posterior standard deviation $\sigma_t(z_n)$ and the number of evaluations $r_n(t)$. Here, the standard deviation represents the *surrogate uncertainty*, and the number of evaluations represents the *evaluation uncertainty* at a certain point. The surrogate uncertainty shrinks globally whenever there are new observations, and the evaluation uncertainty encourages the evaluation of soft z_n ’s that have not been sufficiently evaluated. Furthermore, by specifying different values of β_t , the user can dynamically adjust the weight given to either exploiting known good regions or exploring uncertain ones. This flexibility allows for a

Algorithm 1 General Procedure of the Evaluation and Selection Stage with M-UCB

Input: The feasible set of prompts $\mathcal{Z} = \{z_1, \dots, z_N\}$, a parametric model $\mathbf{f}(\cdot; \mathbf{W})$, a prior distribution of unknown parameters $\pi(\mathbf{W})$, the total budget of evaluating prompts T , and the number of evaluations at each soft prompt R in the warm-up stage.

Output: The selected soft prompt \hat{z}^* .

Warm-Up Step:

- 1: Decide the set of prompts \mathcal{Z}_W to be evaluated in the warm-up step as in Section 4.1.
- 2: **for** $\forall z_{W;n} \in \mathcal{Z}_W$ **do**
- 3: Evaluate $z_{W;n}$ for R times.
- 4: Record the sample variances $\hat{\sigma}_{W;n}^2$.
- 5: **end for**
- 6: Approximate σ_n^2 for $n \in \{1, 2, \dots, N\}$.
- 7: Set $T_W = |\mathcal{Z}_W| R$.

Sequential Evaluation Step:

- 8: Let $t = T_W$ and $\mathcal{S}_t = \{(z^{(1)}, \hat{v}^{(1)}), \dots, (z^{(t)}, \hat{v}^{(t)})\}$.
- 9: **while** $t < T$ **do**
- 10: Update the posterior distribution $p(\mathbf{W} | \mathcal{S}_t)$ as in (5).
- 11: Selecting the next soft prompt $z^{(t+1)}$ by maximizing the M-UCB function

$$z^{(t+1)} \in \arg \max_{z_n \in \mathcal{Z}} \alpha_t(z_n).$$

- 12: Observe $\hat{v}^{(t+1)}$ with $z^{(t+1)}$ as in (4).
 - 13: Update the historical dataset $\mathcal{S}_{t+1} = \{(z^{(t+1)}, \hat{v}^{(t+1)})\} \cup \mathcal{S}_t$ and let $t \leftarrow t + 1$.
 - 14: **end while**
 - 15: **return** $n^* = \arg \max_{n \in \{1, 2, \dots, N\}} \frac{1}{r_n(T)} \sum_{m=1}^{r_n(T)} \hat{v}_{n,m}$ and $\hat{z}^* = z_{n^*}$.
-

more nuanced approach to optimization, compared to the classical acquisition functions including Probability of Improvement and Expected Improvement (Frazier 2018).

We now present the consistency of **Algorithm 1**. We make the following assumptions.

ASSUMPTION 1.

1. For each soft prompt, the mean score is identifiable with different \mathbf{W} 's and the squared mean score is integrable with respect to the prior. That is, $\forall z_n \in \mathcal{Z}, \mathbf{f}(z_n; \mathbf{W}) \neq \mathbf{f}(z_n; \mathbf{W}')$ when $\mathbf{W} \neq \mathbf{W}'$, and $\mathbb{E}_{\mathbf{W} \sim \pi(\mathbf{W})} [\mathbf{f}^2(z_n; \mathbf{W})] < \infty$.

2. For the user-selected hyperparameter β_t , $\lim_{t \rightarrow \infty} \beta_t = \infty$.

THEOREM 1. *Let $z^* \in \arg \max_{z_n \in \mathcal{Z}} v(z_n)$ be the prompt with the highest mean score and \widehat{z}^* be the selected soft prompt by **Algorithm 1**. Under Assumption 1,*

$$\lim_{T \rightarrow \infty} v(\widehat{z}^*) \stackrel{w.p.1}{=} v(z^*).$$

Theorem 1 gives us the consistency of the sequential evaluation step of our framework. The first condition in Assumption 1 appears to be a common assumption used in Bayesian inference to regularize the model; see Van der Vaart (2000) for example. The second condition is commonly employed in the literature related to the Gaussian process and neural network bandit algorithms (Srinivas et al. 2009, Zhou et al. 2020). As $t \rightarrow \infty$, the posterior variance at each $\mathbf{f}(z_n; \widehat{\mathbf{W}})$ shrinks to zero. In this way, the rescaled M-UCB function $\alpha'_t(z_n) = \frac{\mu_t(z_n)}{\beta_t} + \sigma_t(z_n) + \gamma(r_n(t))$ approaches zero if and only if $r_n(t) \rightarrow \infty$. The detailed proof is postponed to the supplements.

When the posterior distribution of the unknown parameters $p(\mathbf{W} | \mathcal{S}_t)$ does not adopt a closed-form expression, it is challenging to obtain the closed-form expression of $\mu_t(z_n)$ and $\sigma_t(z_n)$ as well. In these scenarios, we simulate samples $\widehat{\mathbf{W}}_k \sim p(\mathbf{W} | \mathcal{S}_t)$ for $k = 1, 2, \dots, K$ with a selected sampling algorithm. In this way, for each soft prompt z_n , we have a set of samples $\mathcal{A}_n \doteq \left\{ \mathbf{f}(z_n; \widehat{\mathbf{W}}_1), \mathbf{f}(z_n; \widehat{\mathbf{W}}_2), \dots, \mathbf{f}(z_n; \widehat{\mathbf{W}}_K) \right\}$ to infer the mean score $v(z_n)$. Thus, when optimizing the acquisition function M-UCB (7), we instead consider $\arg \max_{z_n} \{ \widehat{\alpha}_t(z_n) \doteq \widehat{\mu}_t(z_n) + \beta_t(\widehat{\sigma}_t(z_n) + \gamma(r_n(t))) \}$, where

$$\widehat{\mu}_t(z_n) = \frac{1}{K} \sum_{k=1}^K \mathbf{f}(z_n; \widehat{\mathbf{W}}_k), \quad \widehat{\sigma}_t(z_n) = \sqrt{\frac{1}{K-1} \sum_{k=1}^K \left(\mathbf{f}(z_n; \widehat{\mathbf{W}}_k) - \widehat{\mu}_t(z_n) \right)^2} \quad (8)$$

are the sample mean and standard deviation associated with the simulated samples \mathcal{A}_n . Recall that $z^{(t+1)} \in \arg \max_{z_n \in \mathcal{Z}} \alpha_t(z_n)$.

PROPOSITION 1. *Suppose $\widehat{\mathbf{W}}_1, \dots, \widehat{\mathbf{W}}_K \stackrel{i.i.d.}{\sim} p(\mathbf{W} | \mathcal{S}_t)$ and $\max_{z_n \in \mathcal{Z}} \mathbb{E}[f^2(z_n; \mathbf{W}) | \mathcal{S}_t] < \infty$. Let $\bar{z}_t^* \in \arg \max_{z_n \in \mathcal{Z}} \widehat{\alpha}_t(z_n)$. Then*

$$\lim_{K \rightarrow \infty} \widehat{\alpha}_t(\bar{z}_t^*) \stackrel{w.p.1}{=} \alpha_t(z^{(t+1)}).$$

We refer to Asmussen and Glynn (2007) for detailed discussions on practical implementations and theoretical support of algorithms for simulating samples $\widehat{\mathbf{W}}_k$, and provide two specific methods in the supplements.

On the other hand, the number of soft prompts could be large in some scenarios. Thus, it is time-consuming to acquire each \mathcal{A}_n in each round. To alleviate the computational burdens, we employ a probabilistic reparameterization method (Daulton et al. 2022) to optimize the acquisition function. That is, we assign a probability mass function to the feasible set of soft prompts $z_n \sim p(z; \theta)$, where $p(z; \theta)$ is a probability mass function defined on $\mathcal{Z} = \{z_1, z_2, \dots, z_N\}$, and parametrized by a

continuous parameter $\theta \in \Theta$. Specifically, we set $\Theta = [0, 1]^N$ and let $z = z_i$ with probability $\frac{\theta^{(i)}}{\sum_{j=1}^N \theta^{(j)}}$, where $\theta^{(i)}$ denotes the i -th entry of θ . We define

$$\theta_t^* = \arg \max_{\theta \in \Theta} \{ \tilde{\alpha}_t(\theta) \doteq \mathbb{E}_{p(z; \theta)} [\alpha_t(z)] \},$$

which is a continuous optimization problem regarding $\theta \in \Theta$, and can be facilitated efficiently with gradient-based algorithms. After determining θ_t^* , we generate $\hat{z}^{(t+1)} \sim p(z; \theta_t^*)$ and then observe the score associated with $\hat{z}^{(t+1)}$ as in (4).

We name the acquisition function $\tilde{\alpha}_t(\theta)$ *Probabilistic Reparameterized Modified Upper Confidence Bound (PR-M-UCB)*, and provide the theoretical support of using PR-M-UCB.

THEOREM 2. Denote $\mathcal{H}_t^* = \{z \in \arg \max_{z \in \mathcal{Z}} \alpha_t(z)\}$ and $\mathcal{J}_t^* = \{\theta \in \arg \max_{\theta \in \Theta} \tilde{\alpha}_t(\theta)\}, \forall t > 0$. Let

$$\hat{\mathcal{H}}_t^* = \{z : \theta \in \mathcal{J}_t^*, z \in \text{support}(p(z; \theta))\}.$$

Then, $\hat{\mathcal{H}}_t^* = \mathcal{H}_t^*, \forall t > 0$.

Theorem 2 states that the maximizers of PR-M-UCB lead to a probability distribution that generates the maximizers of M-UCB. Specifically, when the maximizer of M-UCB is unique, the maximizers of PR-M-UCB lead to a point mass distribution supported only at the unique maximizer of M-UCB.

The advantage of PR-M-UCB over M-UCB is that the maximization of PR-M-UCB is a continuous optimization problem, which can be facilitated by gradient ascent efficiently and effectively (Robbins and Monro 1951). Indeed, the differentiability of PR-M-UCB is supported by the differentiability of $p(z; \theta)$ with θ , and is formalized into the following proposition.

PROPOSITION 2. $\tilde{\alpha}_t(\theta)$ is differentiable with $\theta \in \Theta$, and the gradient is $\nabla_{\theta} \tilde{\alpha}_t(\theta) = \mathbb{E}_{\nabla_{\theta} p(z; \theta)} [\alpha_t(z)]$.

Furthermore, we provide an unbiased estimator of the gradient with the following proposition.

PROPOSITION 3. An unbiased estimator of the gradient $\nabla_{\theta} \tilde{\alpha}_t(\theta)$ is

$$\widehat{\nabla}_{\theta} \tilde{\alpha}_t(\theta) \doteq \frac{1}{I} \sum_{i=1}^I \alpha_t(\hat{z}_i) \nabla_{\theta} \log(p(\hat{z}_i; \theta)), \quad (9)$$

where $\hat{z}_i \stackrel{i.i.d.}{\sim} p(z; \theta)$ and $p(\hat{z}_i; \theta) > 0$.

The acquisition function $\alpha_t(\hat{z}_i)$ in (9) is approximated by (8). In this way, the stochastic gradient ascent method can be performed to optimize PR-M-UCB with multiple starts. The detailed procedure of the sequential evaluation step with PR-M-UCB is in **Algorithm 2**.

Algorithm 2 Detailed Procedure of Sequential Evaluation Step with PR-M-UCB

Input: The feasible set of prompts $\mathcal{Z} = \{z_1, \dots, z_N\}$, a parametric model $\mathbf{f}(\cdot; \mathbf{W})$, a prior distribution of unknown parameters $\pi(\mathbf{W})$, the total budget of evaluating prompts T , the collected observed scores after the warm-up stage \mathcal{S}_{T_W} , the estimated evaluation uncertainty $\sigma_n^2, n \in \{1, 2, \dots, N\}$, the number of iterations \mathfrak{T} for gradient ascent, the sequence of learning rates $\ell_t, t \in \{1, 2, \dots, \mathfrak{T}\}$, and the number of the starting points \mathfrak{M} for gradient ascent.

Output: The selected soft prompt \hat{z}^* .

- 1: Let $t = T_W$.
- 2: **while** $t < T$ **do**
- 3: Update the posterior distribution $p(\mathbf{W} \mid \mathcal{S}_t)$ as in (5).
- 4: Sample $\widehat{\mathbf{W}}_k \sim p(\mathbf{W} \mid \mathcal{S}_t)$ for $k \in \{1, 2, \dots, K\}$.
- 5: Let $\mathfrak{t} = 0$ and uniformly select $\theta_{\mathfrak{m}}^{(0)} \in \Theta$ in random for $\mathfrak{m} = \{1, 2, \dots, \mathfrak{M}\}$.
- 6: **while** $\mathfrak{t} < \mathfrak{T}$ **do**
- 7: **for** $\mathfrak{m} = \{1, 2, \dots, \mathfrak{M}\}$ **do**
- 8: **for** $i = 1, 2, \dots, I$ **do**
- 9: Sample $\hat{z}_i \sim p(z; \theta_{\mathfrak{m}}^{(\mathfrak{t})})$.
- 10: Estimate $a_{\mathfrak{t}, \mathfrak{m}, i} \doteq \hat{\alpha}_{\mathfrak{t}}(\hat{z}_i)$ with $\left\{ \mathbf{f}(\hat{z}_i; \widehat{\mathbf{W}}_1), \mathbf{f}(\hat{z}_i; \widehat{\mathbf{W}}_2), \dots, \mathbf{f}(\hat{z}_i; \widehat{\mathbf{W}}_K) \right\}$ as in (8).
- 11: **end for**
- 12: Calculate the estimated gradient $\eta = \frac{1}{I} \sum_{i=1}^I a_{\mathfrak{t}, \mathfrak{m}, i} \nabla_{\theta} \log(p(\hat{z}_i; \theta))$.
- 13: Let $\theta_{\mathfrak{m}}^{(\mathfrak{t}+1)} = \theta_{\mathfrak{m}}^{(\mathfrak{t})} + \ell_{\mathfrak{t}} \eta$.
- 14: **end for**
- 15: Let $\mathfrak{t} \rightarrow \mathfrak{t} + 1$.
- 16: **end while**
- 17: Select $\mathfrak{m}^* = \arg \max_{\mathfrak{m} \in \{1, 2, \dots, \mathfrak{M}\}} \sum_{i=1}^I a_{\mathfrak{t}, \mathfrak{m}, i}$.
- 18: Let $\theta_{\mathfrak{t}}^* = \theta_{\mathfrak{m}^*}^{\mathfrak{T}}$.
- 19: Sample $\hat{z}^{(\mathfrak{t}+1)} \sim p(z; \theta_{\mathfrak{t}}^*)$.
- 20: Observe $\hat{v}^{(\mathfrak{t}+1)}$ with $\hat{z}^{(\mathfrak{t}+1)}$ as in (4).
- 21: Update the historical dataset $\mathcal{S}_{\mathfrak{t}+1} = \{(\hat{z}^{(\mathfrak{t}+1)}, \hat{v}^{(\mathfrak{t}+1)})\} \cup \mathcal{S}_{\mathfrak{t}}$.
- 22: Let $t \rightarrow t + 1$.
- 23: **end while**
- 24: **return** $n^* = \arg \max_{n \in \{1, 2, \dots, N\}} \frac{1}{r_n(T)} \sum_{m=1}^{r_n(T)} \hat{v}_{n, m}$ and $\hat{z}^* = z_{n^*}$.

5. Refinement

In this section, we provide a procedure to refine the proposed two-stage framework with the observed scores after completing the evaluation and selection stage. Specifically, we first refine the

projection mapping from the latent space $\tilde{\mathcal{X}} \subseteq \mathbb{R}^{\tilde{D}}$. Recall that each soft prompt $z_n \in \mathcal{Z} \subseteq \mathbb{R}^D$ is attained by projecting a latent vector X_n in the latent vector set \mathcal{X} to $z_n = AX_n$, where A is the projection matrix attained through principal component analysis, as described in Section 3.2. That is, without prior knowledge, we assume that the projection is linear. We then refine the projection mapping based on the scores observed during the evaluation and selection stage, introducing a non-linear mapping $\tilde{A}^*(\cdot) : \mathbb{R}^{\tilde{D}} \rightarrow \mathbb{R}^{D^*}$. This enhances the flexibility of the projection from the latent space. The dimension of the space after this refined projection, denoted as D^* , is not necessarily equivalent to the dimension of the soft prompt space D before the refinement.

We introduce a *projection stochastic kriging* (PSK) model to facilitate the construction of the nonlinear projection mapping $\tilde{A}^*(X)$. We assume that the observed score regarding the latent vector is

$$\hat{v}_m(X) = v(X) + \epsilon_m(X), X \in \tilde{\mathcal{X}}, \quad (10)$$

where

$$v(X) \sim \mathcal{GP}\left(0, \tilde{A}^*(X)^\top \tilde{A}^*(X')\right). \quad (11)$$

Here, $\hat{v}_m(X)$ denotes a score that will be observed when evaluating the human-readable prompt $\mathbf{prom}(X) \doteq \text{Dec}(X)$. That is, given a vector in the latent space $X \in \tilde{\mathcal{X}}$, the decoder model described in Section 3.1 will output a human-readable text, serving as a prompt. In addition, $v(X)$ is the mean score of $\mathbf{prom}(X)$; and $\epsilon_m(X) \stackrel{i.i.d.}{\sim} \mathcal{N}(0, \sigma_\epsilon^2(X))$ is the uncertainty of the scores to be observed when evaluating $\mathbf{prom}(X)$. Furthermore, the mean score regarding the latent vector is a realization from a zero-mean Gaussian process, and the kernel function $\mathbf{K}(X, X') = \tilde{A}^*(X)^\top \tilde{A}^*(X')$ is defined on the latent space $\tilde{\mathcal{X}}$.

We now describe the preparation for learning the projection mapping from the observed scores. Recall that the set of observed scores upon completing the evaluation and selection stage is $\mathcal{S}_T = \{(z_n, \hat{v}_{n,m})\}$ for $m \in \{1, 2, \dots, r_n(T)\}$ and $n \in \{1, 2, \dots, N\}$. Here $z_n \in \mathcal{Z}$ denotes the soft prompt, $\hat{v}_{n,m}$ denotes the m -th observed score when evaluating the prompt associated with z_n , and $r_n(T)$ is the number of evaluations at z_n when the total budget T is reached. Without loss of generality, we assume that $r_n(T) \geq 1$ for $n \in \{1, 2, \dots, N\}$. Each soft prompt z_n has an associated latent vector $X_n \in \mathcal{X} \subseteq \tilde{\mathcal{X}}$. In the remaining part, we consider the set of the observed scores as $\mathcal{S}_T = \{(X_n, \hat{v}_{n,m})\}$. That is, the soft prompts are replaced with the corresponding latent vectors. Regarding the observation uncertainty, we attain the sample variance for each X_n and then construct a predictive model to estimate $\sigma_\epsilon^2(X), X \in \tilde{\mathcal{X}}$, following the method described in Section 4.1.

Let us now consider the learning procedure of the projection mapping \tilde{A}^* through the lens of the PSK model. Note that the kernel function of PSK is the inner product between the projections $\tilde{A}^*(X)$ and $\tilde{A}^*(X')$. Suppose that the refined projection mapping $\tilde{A}^*(\cdot)$ is selected from a known

class of mappings $\tilde{\mathcal{A}}$, such as a neural network model with fixed layers of nodes and unknown weight parameters, and the learning of the refined projection mapping is through

$$\tilde{A}^* = \arg \max_{\tilde{A} \in \tilde{\mathcal{A}}} \ell(\mathcal{S}_T; \tilde{A}),$$

where

$$\ell(\mathcal{S}_T; \tilde{A}) = -\frac{1}{2} \ln \left[\left[\mathbf{K}_N(\tilde{A}) + \boldsymbol{\Sigma}_{\varepsilon;N} \right] - \frac{1}{2} \tilde{\mathbf{V}}_N^\top \left[\mathbf{K}_N(\tilde{A}) + \boldsymbol{\Sigma}_{\varepsilon;N} \right]^{-1} \tilde{\mathbf{V}}_N \right] \quad (12)$$

is the normalized log-likelihood function of an N -dimensional Gaussian distribution. Here $\mathbf{K}_N(\tilde{A}) \in \mathbb{R}^{N \times N}$ is the kernel matrix, of which the (i, j) -th entry is $\tilde{A}(X_i)^\top \tilde{A}(X_j)$; $\boldsymbol{\Sigma}_{\varepsilon;N} = \text{diag} \{ \sigma_\varepsilon^2(X_1)/r_1(T), \dots, \sigma_\varepsilon^2(X_N)/r_N(T) \}$ denotes the observation uncertainty matrix; and $\tilde{\mathbf{V}}_N = (\tilde{v}_1, \dots, \tilde{v}_N)^\top$ is the mean vector of the observed scores, where $\tilde{v}_n = \frac{1}{r_n(T)} \sum_{m=1}^{r_n(T)} \hat{v}_{n,m}$. In this way, the refined projection matrix is learned by maximizing the log-likelihood function through the kernel matrix $\mathbf{K}_N(\tilde{A})$. We note that, instead of a pre-specified kernel function, our PSK model learns a data-driven kernel function using observed scores, thereby enjoying a higher approximation accuracy for the mean score v . Regarding the dimension of the refined soft prompt space D^* , we choose it using the cross-validation method (Stone 1974). That is, we first determine a set of potential D^* 's, denoted by $\mathcal{D}^* = \{D_1^*, \dots, D_q^*\}$. For each $D_l^* \in \mathcal{D}^*$, we randomly select a proportion of the observations $(X_n, \hat{v}_{n,m}) \in \mathcal{S}_T$, say 70%, to construct a PSK model with dimension D_l^* . We then use the remaining 30% of the observations to evaluate the prediction accuracy for the constructed PSK model (Bastos and O'Hagan 2009). The selected D^* is the one that achieves the highest prediction accuracy among those in \mathcal{D}^* .

In addition to the refinement of the projection, the PSK model can also be used to select latent vectors $X \in \tilde{\mathcal{X}}$ when we have additional budgets to evaluate the prompt after the evaluation and selection stage. Without loss of generality, we assume that $I \geq 0$ additional evaluations have been observed associated with different latent vectors, say $\left\{ (\tilde{X}_1, \tilde{v}_1), \dots, (\tilde{X}_I, \tilde{v}_I) \right\}_{i=1}^I$. Here $\tilde{X}_i \notin \mathcal{X}$ is an additional latent vector different from those in the latent vector set decided during the search stage in Section 3, and $\tilde{v}_i = v(\tilde{X}_i) + \varepsilon(\tilde{X}_i)$ is the observed score associated with \tilde{X}_i . We denote the set of additional latent vectors selected to evaluate during the refinement procedure as $\mathcal{R} = \{ \tilde{X}_1, \tilde{X}_2, \dots, \tilde{X}_I \}$. Based on (10) and (11), for any latent vector in the latent space $\forall X \in \tilde{\mathcal{X}}$, we have a PSK predictor for the mean score $v(X)$ as

$$\hat{\mu}(X) = \left(\mathbf{K}_N(X)^\top, \tilde{\mathbf{K}}_I(X)^\top \right) \left(\left(\begin{array}{cc} \mathbf{K}_N & \tilde{\mathbf{K}}_{N,I} \\ \tilde{\mathbf{K}}_{N,I}^\top & \tilde{\mathbf{K}}_I \end{array} \right) + \boldsymbol{\Sigma}_{\varepsilon;N+I} \right)^{-1} \begin{pmatrix} \tilde{\mathbf{V}}_N \\ \tilde{\mathbf{V}}_I \end{pmatrix}, \quad (13)$$

with the associated prediction uncertainty quantified by

$$\widehat{\sigma}^2(X) = \tilde{A}^*(X)^\top \tilde{A}^*(X) - \left(\mathbf{K}_N(X)^\top, \tilde{\mathbf{K}}_I(X)^\top \right) \left(\left(\begin{array}{cc} \mathbf{K}_N & \tilde{\mathbf{K}}_{N,I} \\ \tilde{\mathbf{K}}_{N,I}^\top & \tilde{\mathbf{K}}_I \end{array} \right) + \boldsymbol{\Sigma}_{\varepsilon;N+I} \right)^{-1} \begin{pmatrix} \mathbf{K}_N(X) \\ \tilde{\mathbf{K}}_I(X) \end{pmatrix}. \quad (14)$$

Here

$$\begin{aligned}
\mathbf{K}_N(X) &\in \mathbb{R}^N \text{ with } [\mathbf{K}_N(X)]_i = \tilde{A}^*(X)^\top \tilde{A}^*(X_i) \text{ for } X_i \in \mathcal{X}; \\
\tilde{\mathbf{K}}_I(X) &\in \mathbb{R}^I \text{ with } [\tilde{\mathbf{K}}_I(X)]_i = \tilde{A}^*(X)^\top \tilde{A}^*(\tilde{X}_i) \text{ for } \tilde{X}_i \in \mathcal{R}; \\
\mathbf{K}_N &\in \mathbb{R}^{N \times N} \text{ with } [\mathbf{K}_N]_{i,j} = \tilde{A}^*(X_i)^\top \tilde{A}^*(X_j) \text{ for } X_i, X_j \in \mathcal{X}; \\
\tilde{\mathbf{K}}_I &\in \mathbb{R}^{I \times I} \text{ with } [\tilde{\mathbf{K}}_I]_{i,j} = \tilde{A}^*(\tilde{X}_i)^\top \tilde{A}^*(\tilde{X}_j) \text{ for } \tilde{X}_i, \tilde{X}_j \in \mathcal{R}; \\
\tilde{\mathbf{K}}_{N,I} &\in \mathbb{R}^{N \times I} \text{ with } [\tilde{\mathbf{K}}_{N,I}]_{i,j} = \tilde{A}^*(X_i)^\top \tilde{A}^*(\tilde{X}_j) \text{ for } X_i \in \mathcal{X} \text{ and } \tilde{X}_j \in \mathcal{R}.
\end{aligned}$$

Also, $\Sigma_{\epsilon;N+I} = \text{Diag} \left\{ \sigma_\epsilon^2(X_1)/r_1(T), \dots, \sigma_\epsilon^2(X_N)/r_N(T), \sigma_\epsilon^2(\tilde{X}_1), \dots, \sigma_\epsilon^2(\tilde{X}_I) \right\}$ denotes the observation uncertainty matrix; $\mathbf{V}_N = (\bar{v}_1, \dots, \bar{v}_N)^\top$ is the mean vector of the observed scores as defined in (12); and $\tilde{\mathbf{V}}_I = (\tilde{v}_1, \dots, \tilde{v}_I)^\top$ denotes the observation vector of the additional evaluations.

In this way, the refinement with the PSK model enables an explicit mean score predictor and the prediction uncertainty $\forall X \in \tilde{\mathcal{X}}$ extending beyond the finite set \mathcal{X} determined in the search stage. Consequently, classical simulation experimental designs and simulation optimization methods, particularly those based on the Gaussian process model, can be directly applied to the latent space $\tilde{\mathcal{X}} \subseteq \mathbb{R}^D$. For instance, with an explicit Gaussian process representation for the latent vector $X \in \tilde{\mathcal{X}}$, Bayesian optimization algorithms or Gaussian process search algorithms (Wang et al. 2023) can be employed. These methods aim to identify prompts that may achieve higher mean scores than the current optimal prompt selected at the end of the evaluation and selection stage. We note that this search process can extend beyond the previously selected latent vector set $\mathcal{X} = \{X_1, \dots, X_N\}$. Additionally, the proposed PSK model can quantify the uncertainty of observed scores when the input latent vector \hat{X} to the PSK model is itself a random vector. For detailed procedures on employing the stochastic kriging model for input uncertainty analysis, we refer to Xie et al. (2014), Barton et al. (2014). In general, suppose we select a set of $\mathcal{R} = \{\tilde{X}_1, \tilde{X}_2, \dots, \tilde{X}_I\}$ as the additional latent vectors to evaluate with $I \geq 2$, and $\tilde{X}_i \neq \tilde{X}_j$ for $i \neq j$. We consider the *cumulative uncertainty*

$$U_I = \sum_{i=1}^I \widehat{\sigma}^2(\tilde{X}_i), \quad (15)$$

where $\widehat{\sigma}^2(\tilde{X}_i)$ denotes the uncertainty (14) associated with the PSK predictor (13). To provide the upper bound of the cumulative uncertainty, we make the following assumptions.

ASSUMPTION 2.

1. The norm of the refined projection mapping is finite, that is, $\sup_{X \in \tilde{\mathcal{X}}} \|\tilde{A}^*(X)\| < \infty$.
2. The uncertainty in observed scores satisfies $\sigma_\epsilon^2(X) \in \left(\underline{\sigma}_\epsilon^2, \overline{\sigma}_\epsilon^2\right), \forall X \in \tilde{\mathcal{X}}$, where $0 < \underline{\sigma}_\epsilon^2, \overline{\sigma}_\epsilon^2 < \infty$.

THEOREM 3. *Under Assumption 2, the cumulative uncertainty of the PSK predictor*

$$U_I \leq CD^* \log I.$$

Here U_I is the cumulative uncertainty defined in (15); D^* is the dimension of the refined projected space; I denotes the number of additional evaluations in the refinement stage; and C is a constant that does not depend on D^* or I .

Theorem 3 establishes that the cumulative uncertainty increases logarithmically in I . Specifically, the mean uncertainty, represented as $\bar{U}_I = U_I/I$, shrinks to zero as I approaches infinity. Moreover, U_I increases in the dimension of the refined projected space D^* rather than the dimension of the original latent space D . In essence, the projection mapping $\tilde{A}^*(\cdot)$ reduces the uncertainty in approximating the mean score v .

Given that the PSK model approximates the mean score from the latent space \mathcal{X} , a question arises: Why not directly employ the PSK model as a surrogate to facilitate sequential evaluation in selecting prompts within the latent space, rather than using the soft prompt set? The answer consists of two key points: **1. Insufficient observations:** For accurate learning, the PSK model requires a considerable number of observed scores. This requirement is satisfied after the evaluation and selection stage, if sufficient observations are collected. However, it is challenging to have sufficient observations during the evaluation and selection stage. Our proposed framework, as detailed in Section 4, relies on a surrogate model in a moderately-dimensional vector space, which generally needs fewer observations to satisfactorily approximate the mean score. A PSK model with insufficient observations leads to significant uncertainty in the mean score approximation, adversely affecting the evaluation and selection stage. **2. Inefficient evaluations within a continuous space:** In the search stage described in Section 3, we form a set of soft prompts, each representing a distinct, human-readable prompt. By optimizing over this discrete set, we avoid the inefficiency of evaluating similar prompts. In contrast, optimizing directly over the continuous latent space \tilde{X} might result in choosing latent vectors that are closely clustered in a specific region of the space, representing similar prompts. This over-exploitation of a narrow range in the latent space is inefficient. We compare our framework with a sequential evaluation procedure directly utilizing the PSK model, and the numerical results presented in the experimental section support our two-stage framework.

6. Experiments

In this section, we present the numerical experiments of our proposed framework for selecting prompts. For our evaluation, we have chosen GPT-3.5-turbo and text-davinci-003; details can be found at <https://platform.openai.com/docs/models>. The tasks assigned to the selected LLMs

include: Word sorting: 1) Given a list of words as input, output the sorted list in alphabetical order; 2) Rhymes: Given a word A and a list of words, output the word from the list that rhymes with A ; 3) First letter: Given a word as input, output its first letter; 4) Largest animals: Given a list of animals, identify the largest animal; 5) Nums to verbal: Convert a numerical number to its English word form; 6) Count objectives: Given a list of objectives, output the number of objectives in the list. In all experiments, the dimension of the latent space is $\tilde{D} = 3584(7 \times 512)$, and the soft prompt’s dimension is $D = 50$. The number of prompts to select from and the total budget for evaluation will be specified in each experiment. Our experiments were conducted with Pytorch and Python 3.9 on a computer equipped with two AMD Ryzen Threadripper 3970X 32-Core Processors, 256 GB memory, and two Nvidia GeForce RTX 3090 GPUs with 24GB of RAM each. The experimental results presented here are mean performances based on 15 repetitions, with standard deviations represented by a shadow on the mean-value line.

In Section 6.1, we employ different Bayesian parametric models as the surrogate model used to approximate the mean score regarding each soft prompt and compare their approximation accuracy. In Section 6.2, we focus on the sequential evaluation step in the evaluation and selection stage, and compare the optimization procedure with the proposed acquisition functions 1) modified upper confidence bound (M-UCB) and 2) probabilistic reparametrization modified upper confidence bound (PR-M-UCB). In Section 6.3, we compare our two-stage framework with the direct search in the latent space using the projection stochastic kriging (PSK) model.

6.1. Surrogate Model Comparison

In this section, we conduct numerical experiments to compare different surrogate models on approximating the mean score with respect to soft prompts. Specifically, we select 1) a Bayesian linear regression model (BLR), 2) a Gaussian process (GP), 3) a Bayesian neural network (BNN), and 4) a variational autoencoder (VAE). We postpone the detailed descriptions of these surrogate models to the supplements. These selected surrogate models are all represented by a general parametric form $\mathbf{f}(z; \mathbf{W})$, where z is the soft prompt and $\mathbf{W} \subseteq \mathbb{R}^D$ is the unknown parameter of the surrogate model assigned with a prior distribution $\mathbf{W} \sim \pi(\mathbf{W})$. In this set of experiments, the prior distribution for each surrogate model is set as the independent standard normal distribution.

For each set of experiments, we first fix a soft prompt set $\mathcal{Z} = \{z_1, z_2, \dots, z_N\}$. We then randomly select $N_{\text{tr}} = 0.7N$ soft prompts from \mathcal{Z} with equal probabilities, and denote the set of selected soft prompts as \mathcal{Z}_{tr} . For each $z_n \in \mathcal{Z}_{\text{tr}}$, we observe the scores as in (4) for 5 times. We denote the training set as $\mathcal{S}_{\text{tr}} = \{(z_n, \hat{v}_{n,m})\}$ for $m \in \{1, 2, \dots, 5\}$ for $z_n \in \mathcal{Z}_{\text{tr}}$, where $\hat{v}_{n,m}$ denotes the m -th observation of the score evaluating with the soft prompt z_n . We let $\mathcal{Z}_{\text{test}} = \mathcal{Z} \setminus \mathcal{Z}_{\text{tr}}$. For each $z_n \in \mathcal{Z}_{\text{test}}$, we evaluate it and observe the scores for $\tilde{r} = 50$ times. We let $\mathcal{S}_{\text{test}} = \{(z_n, \bar{v}_n)\}$ for $z_n \in \mathcal{Z}_{\text{test}}$ and

$\bar{v}_n = \frac{1}{\bar{r}} \sum_{m=1}^{\bar{r}} \hat{v}_{n,m}$, the sample mean of the observed score. In each set of experiments, we use the same training set \mathcal{S}_{tr} to calculate the posterior distribution of the unknown parameter $p(\mathbf{W} | \mathcal{S}_{\text{tr}})$ as in (5). We then generate $\{\widehat{\mathbf{W}}_1, \widehat{\mathbf{W}}_2, \dots, \widehat{\mathbf{W}}_K\}$ from the posterior distribution $p(\mathbf{W} | \mathcal{S}_{\text{tr}})$, where $K = 100$. Regarding the comparison metric of the surrogate models' performances, we consider 1) root mean squared error (RMSE) and 2) covering ratio (CR). That is

$$\text{RMSE} = \sqrt{\frac{1}{N_{\text{test}}} \sum_{z_n \in \mathcal{Z}_{\text{test}}} (\hat{\mu}(z_n) - \bar{v}_n)^2}, \quad \text{CR} = \frac{1}{N_{\text{test}}} \sum_{z_n \in \mathcal{Z}_{\text{test}}} \mathbb{I}\{\bar{v}_n \in [\mathcal{L}_n, \mathcal{U}_n]\},$$

where $\hat{\mu}(z_n) = \frac{1}{K} \sum_{k=1}^K \mathbf{f}(z_n; \widehat{\mathbf{W}}_k)$ and $[\mathcal{L}_n, \mathcal{U}_n]$ is the 90%-sample quantile of $\{\mathbf{f}(z_n; \widehat{\mathbf{W}}_k)\}_{k=1}^K$. We also consider the impact of the sample size on the surrogate models' performances, with $N \in \{50, 100, 200, 500\}$.

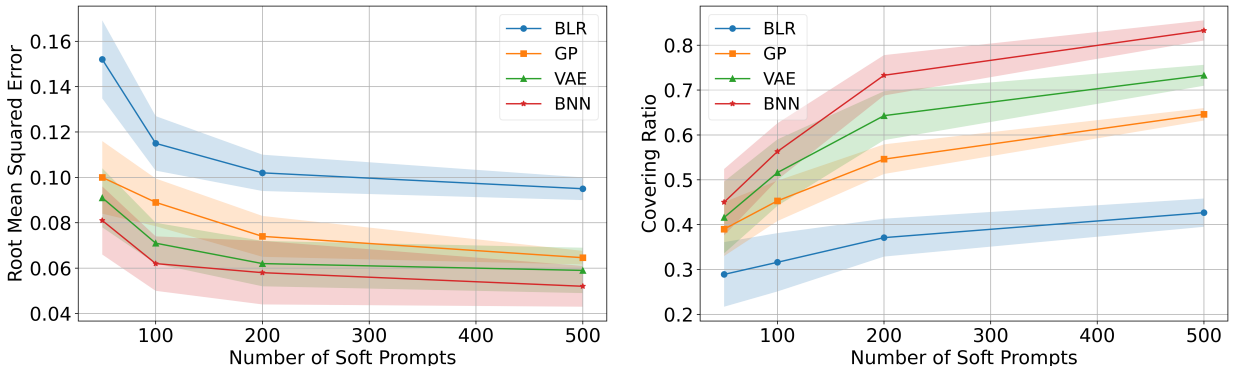


Figure 3 Experimental results for approximating the mean score with the soft prompts using different Bayesian parametric models. The task is word sorting and the generative language model is text-davinci-003.

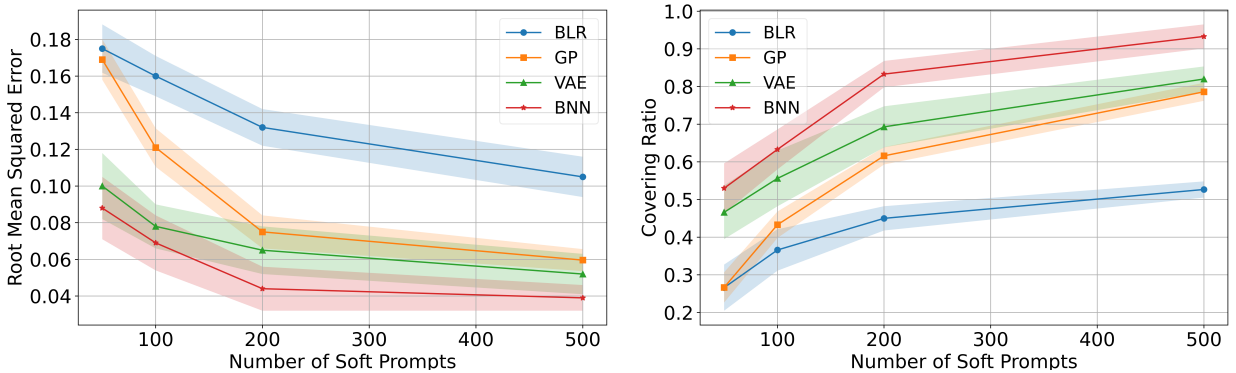


Figure 4 Experimental results for approximating the mean score with the soft prompts using different Bayesian parametric models. The task is word sorting and the generative language model is gpt-3.5-turbo.

The experiment results in **Figure 3** and **Figure 4** provide the following insights on the comparison among surrogate models. First, when there are not sufficient observations to construct the surrogate model ($N = 50$), the difference in the performances of surrogate models on MSE and CR is not significant. In general, these surrogate models all result in relatively high approximation error (indicated by high MSE) and biased approximation confidence (indicated by low CR). This illustrates that constructing a surrogate model for appropriate use requires sufficient observations. Second, as the number of observed scores increases, all the surrogate models achieve better approximation performances, indicated by lower MSE and higher CR. On the other hand, the improvement in the BLR model’s performance is not as significant as in other models. That is, BLR cannot capture the dependence of the mean score on the soft prompt because of the lack of expressive power. Lastly, among all experiments, BNN achieves the best performance with the lowest MSE and highest CR. This is due to BNN’s greater flexibility and expressiveness compared to BLR and GP, and its strong approximation power to capture the highly non-structural dependence of the mean score on the soft prompt. On the other hand, VAE, as another deep learning model, does not perform as well as BNN in our experiments. This is because VAE has a much more complex model structure and generally requires more data (observations of scores in our experiments) to train. In our experiments, even when $N = 500$, the observations are not sufficient to train a VAE model. For these reasons, we select BNN as the surrogate model for approximating the mean score function in the following experiments.

6.2. Acquisition Function Optimization

In this section, we compare the two acquisition functions used in the sequential evaluation step in our framework: M-UCB and PR-M-UCB. Recall that M-UCB is $\alpha_t(z_n) = \mu_t(z_n) + \beta_t(\sigma_t(z_n) + \gamma(r_n(t)))$, where $\mu_t(z_n)$ and $\sigma_t(z_n)$ are the posterior mean and standard deviation of the surrogate model at z_n , and $r_n(t)$ denotes the number of evaluations at z_n up to time t . In this set of experiments, we set $\beta_t = \sqrt{2\log(t)}$ and $\gamma(m) = 2m^{-1/2}$. Since maximizing M-UCB requires evaluating each $z_n \in \mathcal{Z}$, when the total number of soft prompts N is large, it is time-consuming to select the next soft prompt to evaluate. We also consider maximizing PR-M-UCB $\tilde{\alpha}_t(\theta) \doteq \mathbb{E}_{p(z_n; \theta)}[\alpha_t(z_n)]$, where $p(z_n)$ is a categorical distribution as described in Section 4.2.2. Since it is a continuous optimization problem θ , we employ the method of gradient ascent with multiple starting points. Specifically, the algorithm using the gradient descent method is represented by PR-M-UCB $(\mathfrak{M}, \mathfrak{T})$, where \mathfrak{M} is the number of starting points and \mathfrak{T} is the number of gradient ascent iterations.

We consider different numbers of the soft prompts $N \in \{200, 500, 800, 1000\}$. The total budget is fixed as $T = 500$. We select BNN as the surrogate model and use variational inference (VI) to

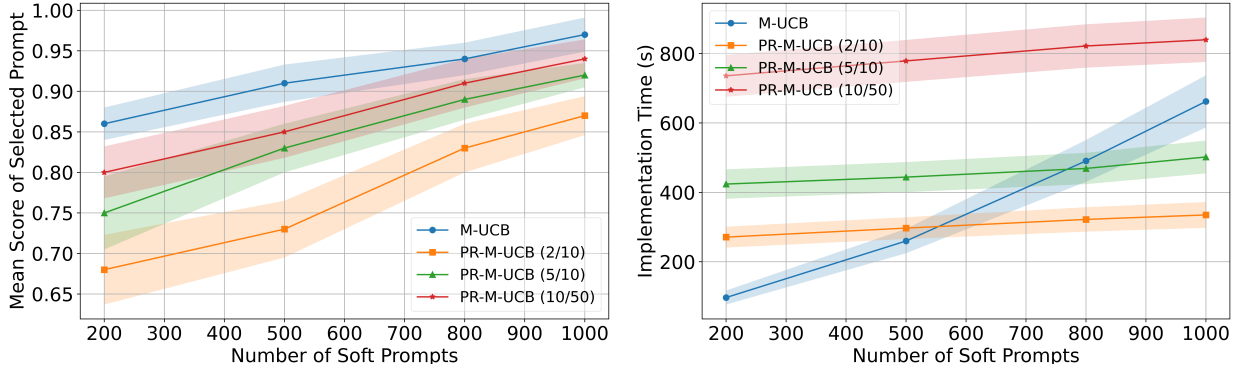


Figure 5 Experimental results for comparison between two acquisition functions: M-UCB and PR-M-UCB (number of starting points, number of gradient ascent iterations). The task is finding the largest animals given the names and the generative language model is gpt-3.5-turbo.

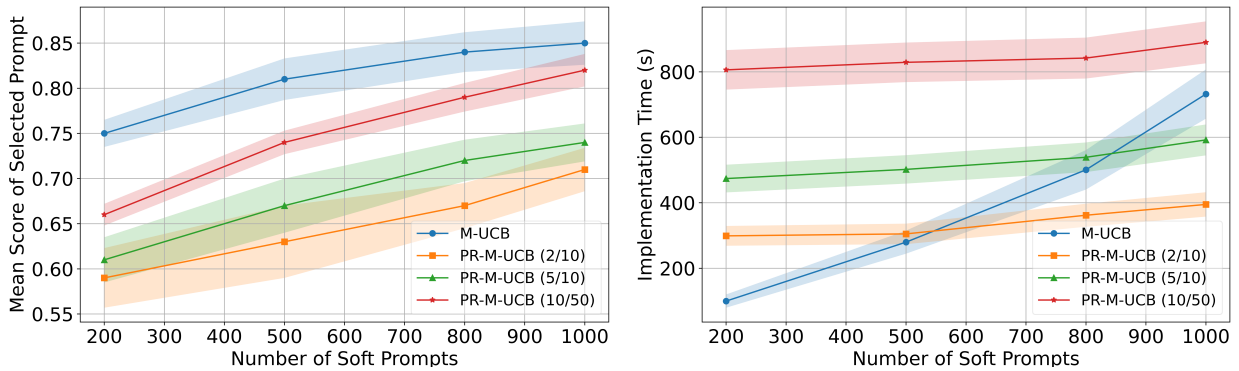


Figure 6 Experimental results for comparison between two acquisition functions: M-UCB and PR-M-UCB (number of starting points, number of gradient ascent iterations). The task is word sorting and the generative language model is text-davinci-003.

generate unknown parameters $\{\widehat{\mathbf{W}}_k\}_{k=1}^{100}$. In the warm-up step, we randomly select $N_W = 0.05N$ soft prompts with equal probabilities and evaluate each soft prompt 5 times. The compared methods use a same BNN at the beginning of the sequential evaluation step. Regarding the comparing metric, we record the mean score of the selected prompt when the total budget is used up. The mean score of the selected prompt is approximated by additionally evaluating it for 50 times. We also record the implementation time of the methods during the sequential evaluation step, which includes the time for updating the surrogate model, generating unknown parameters from the posterior distribution, and optimizing the acquisition function.

The experiment results contained in **Figure 5** and **Figure 6** provide insights as follows. First, M-UCB achieves higher scores than PR-M-UCB across all sets of experiments, since M-UCB evaluates all soft prompts in each iteration. Second, the performance of PR-M-UCB improves as the number

of iterations and starting points in the gradient ascent algorithm increase. Third, the implementation time of M-UCB increases almost linearly with the number of soft prompts. In contrast, the implementation time of PR-M-UCB is determined by the settings of the gradient ascent algorithm, specifically the number of iterations and starting points. As the number of soft prompts increases, the implementation time of PR-M-UCB does not increase significantly. Considering both algorithm performance and implementation time, we recommend using M-UCB for a smaller number of soft prompts, and switching to PR-M-UCB when the number of soft prompts is large.

6.3. Two-stage Framework v.s. Latent Space Searching

In this section, we conduct numerical experiments to compare our proposed two-stage framework with the approach that directly evaluates and selects latent vectors. Recall that the projection stochastic kriging (PSK) model provides an approximation directly from the latent vector $X \in \tilde{\mathcal{X}}$ to the mean score. As a Gaussian process model, the PSK model is compatible with classical simulation optimization methods. In this set of experiments, we employ the acquisition function expected improvement (EI) (see [Frazier \(2018\)](#)), and regard every observation of the score as deterministic without noise. Specifically, in each iteration t , the latent vector to evaluate is selected by maximizing

$$\text{EI}_t(X) = (\hat{\mu}(X) - v_t^*) \Phi \left(\frac{\hat{\mu}(X) - v_t^*}{\sqrt{\hat{\sigma}^2(X)}} \right) + \sqrt{\hat{\sigma}^2(X)} \phi \left(\frac{\hat{\mu}(X) - v_t^*}{\sqrt{\hat{\sigma}^2(X)}} \right) \quad (16)$$

Here Φ and ϕ are the cumulative distribution function and the probability density function of the standard normal distribution; v_t^* is the highest observed score up to time t ; $\hat{\mu}(X)$ and $\hat{\sigma}^2(X)$ denote the PSK predictor and the associated prediction uncertainty as described in (13) and (14). We denote the direct search in the latent space using the PSK model and the EI function as PSK-EI.

In comparison, we implement our proposed two-stage framework and employ the acquisition function M-UCB. We consider different total budgets as $T \in \{50, 200, 500, 1000\}$. In terms of the search stage, we construct a set of $N = 200$ soft prompts for all sets of experiments. In addition, we also consider the refinement procedure of our framework. That is, after the total budget is used up, we construct a PSK model using the observations and search within the latent space using the EI function (16) with 20 additional evaluations. We denote this method as M-UCB-r in the experimental results. Regarding PSK-EI and M-UCB, we record the mean score of the selected prompt when the total budget is used up. For M-UCB-r, we record the mean score when the additional evaluations are used up as well. The mean score of the selected prompt is approximated by additionally evaluating it more 50 times.

The experimental results contained in **Figure 7** provide following insights. First, in all sets of experiments, our proposed two-stage framework achieves higher scores than direct search in the

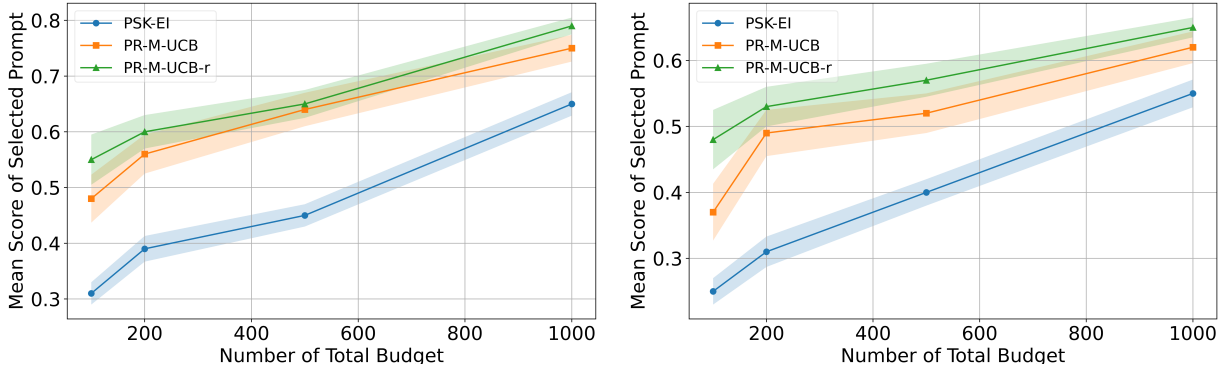


Figure 7 Experimental results for comparison between the proposed two-stage framework and the direct search in the latent space with PSK. The pair of task and generative language model includes 1) counting the objectives with gpt-3.5-turbo (left) and 2) finding the rhymes with text-davinci-003 (right).

high-dimensional latent space using PSK. This is because the PSK model requires sufficient observations to construct an accurate surrogate model. During the sequential evaluation and selection without sufficient observations, the constructed PSK model often fails to provide a satisfactory approximation of the mean score for the latent vector, thereby not always selecting the prompts that are worth evaluating. Second, as the total budget increases, the improvement in direct search within the latent space is more significant than that of our two-stage framework. This is due to the increasingly accurate approximation provided by PSK, which depends on the number of observations. In comparison, since our two-stage framework is restricted to a finite set of constructed soft prompts, its improvement is relatively limited. Lastly, our two-stage framework benefits from the refinement step with additional evaluations. That is, the score of the selected soft prompt is enhanced after refinement using PSK. On the other hand, this benefit raises a question: if we allocate our total budget to 1) the budget for the two-stage framework and 2) the budget for additional evaluations after the two-stage framework, will there be an enhancement in the scores of the selected prompts? We leave this question for future work. At the end of this section, we provide a summary result of comparison between our two-stage framework and direct search in the latent space in **Figure 8**, which includes all six tasks implemented by the generative language model gpt-3.5-turbo. The experimental results support the use of our two-stage framework, and the selected prompts that achieves the highest mean score are included in the supplements.

7. Conclusion

In this work, we facilitate the selection of language prompts for generative language models using simulation optimization methods. We conclude by pointing out limitations and some future work of this work. In the initial search stage, the latent space of the prompts is decided by the text

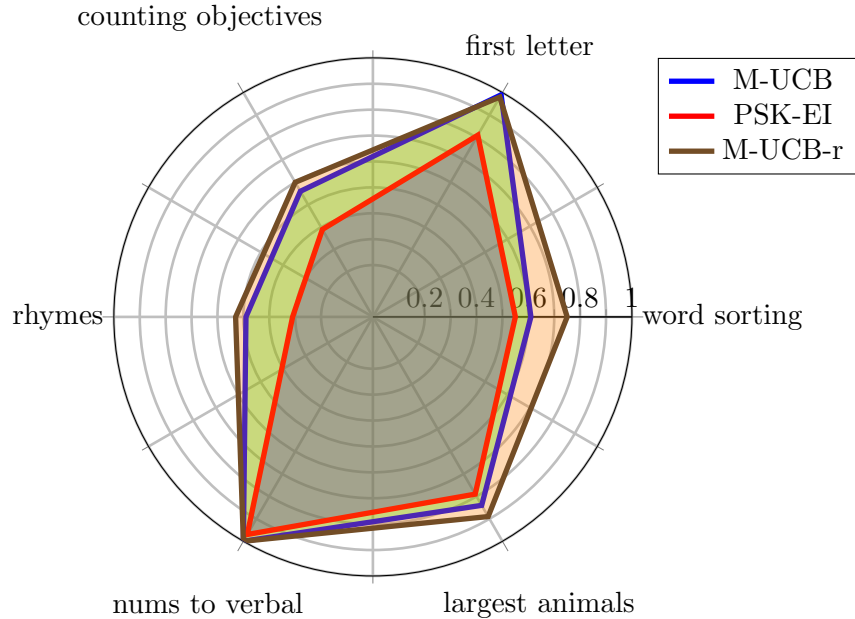


Figure 8 The mean score of the selected prompts in six tasks. The generative language model used to implement the tasks is gpt-3.5-turbo. The total budget is $T = 500$.

autoencoder. Although the text autoencoder has achieved empirical success in practice, it lacks theoretical guarantees due to its complex structure. This limitation presents a challenge in proving theoretical results for the entire framework. Additionally, in our experiments, we observe that the proposed refinement procedure enhances the performance of our two-stage framework when additional budgets are available for evaluating prompts. This raises the question of how to allocate the total budget between the evaluation and selection stage, and the refinement procedure. We defer this discussion to future work.

References

- Ahamed, T. I., Borkar, V. S., and Juneja, S. (2006). Adaptive importance sampling technique for Markov chains using stochastic approximation. *Operations Research*, 54(3):489–504.
- Ankenman, B., Nelson, B. L., and Staum, J. (2010). Stochastic kriging for simulation metamodeling. *Operations Research*, 58(2):371–382.
- Asmussen, S. and Glynn, P. W. (2007). *Stochastic simulation: algorithms and analysis*, volume 57. Springer.
- Ata, B., Harrison, J. M., and Si, N. (2023a). Drift control of high-dimensional rbm: A computational method based on neural networks. *arXiv preprint arXiv:2309.11651*.
- Ata, B., Harrison, J. M., and Si, N. (2023b). Singular control of (reflected) brownian motion: A computational method suitable for queueing applications. *arXiv preprint arXiv:2312.11823*.
- Barton, R. R., Nelson, B. L., and Xie, W. (2014). Quantifying input uncertainty via simulation confidence intervals. *INFORMS Journal on Computing*, 26(1):74–87.

- Bastos, L. S. and O'Hagan, A. (2009). Diagnostics for Gaussian process emulators. Technometrics, 51(4):425–438.
- Blanchet, J., Murthy, K., and Zhang, F. (2022). Optimal transport-based distributionally robust optimization: Structural properties and iterative schemes. Mathematics of Operations Research, 47(2):1500–1529.
- Blei, D. M., Kucukelbir, A., and McAuliffe, J. D. (2017). Variational inference: A review for statisticians. Journal of the American statistical Association, 112(518):859–877.
- Bro, R. and Smilde, A. K. (2014). Principal component analysis. Analytical methods, 6(9):2812–2831.
- Chandrasekaran, D. and Mago, V. (2021). Evolution of semantic similarity—a survey. ACM Computing Surveys (CSUR), 54(2):1–37.
- Chen, L., Chen, J., Goldstein, T., Huang, H., and Zhou, T. (2023). Instructzero: Efficient instruction optimization for black-box large language models. arXiv preprint arXiv:2306.03082.
- Chen, X., Ankenman, B. E., and Nelson, B. L. (2012). The effects of common random numbers on stochastic kriging metamodels. ACM Transactions on Modeling and Computer Simulation (TOMACS), 22(2):1–20.
- Chen, X., Ankenman, B. E., and Nelson, B. L. (2013). Enhancing stochastic kriging metamodels with gradient estimators. Operations Research, 61(2):512–528.
- Chowdhery, A., Narang, S., Devlin, J., Bosma, M., Mishra, G., Roberts, A., Barham, P., Chung, H. W., Sutton, C., Gehrmann, S., et al. (2023). Palm: Scaling language modeling with pathways. Journal of Machine Learning Research, 24(240):1–113.
- Church, K. W. (2017). Word2vec. Natural Language Engineering, 23(1):155–162.
- Cover, T. M. (1999). Elements of information theory. John Wiley & Sons.
- Daulton, S., Wan, X., Eriksson, D., Balandat, M., Osborne, M. A., and Bakshy, E. (2022). Bayesian optimization over discrete and mixed spaces via probabilistic reparameterization. Advances in Neural Information Processing Systems, 35:12760–12774.
- De Andrade, I. M. and Tumelero, C. (2022). Increasing customer service efficiency through artificial intelligence chatbot. Revista de Gestão, 29(3):238–251.
- Deo, A. and Murthy, K. (2023). Achieving efficiency in black-box simulation of distribution tails with self-structuring importance samplers. Operations Research.
- Ding, L. and Zhang, X. (2022). Sample and computationally efficient stochastic kriging in high dimensions. Operations Research.
- Dong, J., Feng, M. B., and Nelson, B. L. (2018). Unbiased metamodeling via likelihood ratios. In 2018 Winter Simulation Conference (WSC), pages 1778–1789. IEEE.

-
- Dong, J. and Zhu, Y. (2016). Three asymptotic regimes for ranking and selection with general sample distributions. In 2016 Winter Simulation Conference (WSC), pages 277–288. IEEE.
- Eckman, D. J., Henderson, S. G., and Shashaani, S. (2023a). Diagnostic tools for evaluating and comparing simulation-optimization algorithms. INFORMS Journal on Computing, 35(2):350–367.
- Eckman, D. J., Henderson, S. G., and Shashaani, S. (2023b). Simopt: A testbed for simulation-optimization experiments. INFORMS Journal on Computing, 35(2):495–508.
- Eckman, D. J., Plumlee, M., and Nelson, B. L. (2022). Plausible screening using functional properties for simulations with large solution spaces. Operations Research, 70(6):3473–3489.
- Fan, Q. and Hu, J. (2018). Surrogate-based promising area search for lipschitz continuous simulation optimization. INFORMS Journal on Computing, 30(4):677–693.
- Fan, W., Hong, L. J., and Nelson, B. L. (2016). Indifference-zone-free selection of the best. Operations Research, 64(6):1499–1514.
- Fan, W., Hong, L. J., and Zhang, X. (2020). Distributionally robust selection of the best. Management Science, 66(1):190–208.
- Frazier, P. I. (2018). Bayesian optimization. In Recent advances in optimization and modeling of contemporary problems, pages 255–278. Informs.
- Fu, M. C., Hu, J.-Q., Chen, C.-H., and Xiong, X. (2007). Simulation allocation for determining the best design in the presence of correlated sampling. INFORMS Journal on Computing, 19(1):101–111.
- Garling, D. J. (2007). Inequalities: a journey into linear analysis. Cambridge University Press.
- Ginglinger, E. and Moreau, Q. (2023). Climate risk and capital structure. Management Science, 69(12):7492–7516.
- Giray, L. (2023). Prompt engineering with chatgpt: a guide for academic writers. Annals of biomedical engineering, 51(12):2629–2633.
- Girolami, M. and Calderhead, B. (2011). Riemann manifold langevin and hamiltonian monte carlo methods. Journal of the Royal Statistical Society Series B: Statistical Methodology, 73(2):123–214.
- Glynn, P. W. and Olvera-Cravioto, M. (2019). Likelihood ratio gradient estimation for steady-state parameters. Stochastic Systems, 9(2):83–100.
- Gordy, M. B. and Juneja, S. (2010). Nested simulation in portfolio risk measurement. Management Science, 56(10):1833–1848.
- He, D., Chick, S. E., and Chen, C.-H. (2007). Opportunity cost and ooba selection procedures in ordinal optimization for a fixed number of alternative systems. IEEE Transactions on Systems, Man, and Cybernetics, Part C (Applications and Reviews), 37(5):951–961.
- He, S., Jiang, G., Lam, H., and Fu, M. C. (2023). Adaptive importance sampling for efficient stochastic root finding and quantile estimation. Operations Research.

- Hong, L. J., Fan, W., and Luo, J. (2021). Review on ranking and selection: A new perspective. Frontiers of Engineering Management, 8(3):321–343.
- Hong, L. J., Jiang, G., and Zhong, Y. (2022). Solving large-scale fixed-budget ranking and selection problems. INFORMS Journal on Computing, 34(6):2930–2949.
- Hong, L. J. and Zhang, X. (2021). Surrogate-based simulation optimization. In Tutorials in Operations Research: Emerging Optimization Methods and Modeling Techniques with Applications, pages 287–311. INFORMS.
- Horvitz, E. (2023). The power of prompting.
- Hou, C., Zhu, G., Zheng, J., Zhang, L., Huang, X., Zhong, T., Li, S., Du, H., and Ker, C. L. (2024). Prompt-based and fine-tuned gpt models for context-dependent and-independent deductive coding in social annotation. In Proceedings of the 14th Learning Analytics and Knowledge Conference, pages 518–528.
- Ibrahim, R., Regnard, N., L’Ecuyer, P., and Shen, H. (2012). On the modeling and forecasting of call center arrivals. In Proceedings of the 2012 Winter Simulation Conference (WSC), pages 1–12. IEEE.
- Ibrahim, R. and Whitt, W. (2010). Delay predictors for customer service systems with time-varying parameters. In Proceedings of the 2010 Winter Simulation Conference, pages 2375–2386. IEEE.
- Jiang, G., Hong, L. J., and Nelson, B. L. (2020). Online risk monitoring using offline simulation. INFORMS Journal on Computing, 32(2):356–375.
- Kanter, B. and Fine, A. H. (2022). The Smart Nonprofit: Staying Human-centered in an Automated World. John Wiley & Sons, Incorporated.
- Kim, J., Kong, J., and Son, J. (2021). Conditional variational autoencoder with adversarial learning for end-to-end text-to-speech. In International Conference on Machine Learning, pages 5530–5540. PMLR.
- Kingma, D. P., Welling, M., et al. (2019). An introduction to variational autoencoders. Foundations and Trends® in Machine Learning, 12(4):307–392.
- L. Salemi, P., Song, E., Nelson, B. L., and Staum, J. (2019). Gaussian Markov random fields for discrete optimization via simulation: Framework and algorithms. Operations Research, 67(1):250–266.
- Lam, H. and Li, F. (2022). General feasibility bounds for sample average approximation via vavnik–chervonenkis dimension. SIAM Journal on Optimization, 32(2):1471–1497.
- Li, J., Luong, M.-T., and Jurafsky, D. (2015). A hierarchical neural autoencoder for paragraphs and documents. arXiv preprint arXiv:1506.01057.
- Li, Z., Fan, W., and Hong, L. J. (2023). The (surprising) sample optimality of greedy procedures for large-scale ranking and selection. arXiv preprint arXiv:2303.02951.
- Louveaux, F. V. and Schultz, R. (2003). Stochastic integer programming. Handbooks in operations research and management science, 10:213–266.

-
- Luo, J., Hong, L. J., Nelson, B. L., and Wu, Y. (2015). Fully sequential procedures for large-scale ranking-and-selection problems in parallel computing environments. Operations Research, 63(5):1177–1194.
- Miller, J. W. (2018). A detailed treatment of doob’s theorem. arXiv preprint arXiv:1801.03122.
- Minka, T. (2000). Bayesian linear regression. Technical report, Citeseer.
- Montero, I., Pappas, N., and Smith, N. A. (2021). Sentence bottleneck autoencoders from transformer language models. arXiv preprint arXiv:2109.00055.
- Negoescu, D. M., Frazier, P. I., and Powell, W. B. (2011). The knowledge-gradient algorithm for sequencing experiments in drug discovery. INFORMS Journal on Computing, 23(3):346–363.
- Ni, E. C., Ciocan, D. F., Henderson, S. G., and Hunter, S. R. (2017). Efficient ranking and selection in parallel computing environments. Operations Research, 65(3):821–836.
- OpenAI (2023). Chatgpt. <https://openai.com/blog/chatgpt>.
- Pei, L., Nelson, B. L., and Hunter, S. R. (2022). Parallel adaptive survivor selection. Operations Research.
- Peng, Y., Xiao, L., Heidergott, B., Hong, L. J., and Lam, H. (2022). A new likelihood ratio method for training artificial neural networks. INFORMS Journal on Computing, 34(1):638–655.
- Pryzant, R., Iter, D., Li, J., Lee, Y. T., Zhu, C., and Zeng, M. (2023). Automatic prompt optimization with” gradient descent” and beam search. arXiv preprint arXiv:2305.03495.
- Quan, N., Yin, J., Ng, S. H., and Lee, L. H. (2013). Simulation optimization via kriging: a sequential search using expected improvement with computing budget constraints. Iie Transactions, 45(7):763–780.
- Robbins, H. and Monro, S. (1951). A stochastic approximation method. The annals of mathematical statistics, pages 400–407.
- Rouder, J. N. and Lu, J. (2005). An introduction to Bayesian hierarchical models with an application in the theory of signal detection. Psychonomic bulletin & review, 12(4):573–604.
- Sautner, Z., Van Lent, L., Vilkov, G., and Zhang, R. (2023). Pricing climate change exposure. Management Science.
- Semelhago, M., Nelson, B. L., Song, E., and Wächter, A. (2021). Rapid discrete optimization via simulation with Gaussian Markov random fields. INFORMS Journal on Computing, 33(3):915–930.
- Shen, H., Hong, L. J., and Zhang, X. (2018). Enhancing stochastic kriging for queueing simulation with stylized models. IIE Transactions, 50(11):943–958.
- Skiles, M. (2023). Ai for nonprofits: How to use artificial intelligence for good. <https://donorbox.org/nonprofit-blog/ai-for-nonprofits>. Accessed: 2023-12-27.
- Spangher, A., Ren, X., May, J., and Peng, N. (2022). Newsedits: A news article revision dataset and a novel document-level reasoning challenge. In Proceedings of the 2022 Conference of the North American Chapter of the Association for Computational Linguistics: Human Language Technologies, pages 127–157.

- Srinivas, N., Krause, A., Kakade, S. M., and Seeger, M. (2009). Gaussian process optimization in the bandit setting: No regret and experimental design. arXiv preprint arXiv:0912.3995.
- Stone, M. (1974). Cross-validated choice and assessment of statistical predictions. Journal of the royal statistical society: Series B (Methodological), 36(2):111–133.
- Toutanova, K., Brockett, C., Tran, K. M., and Amershi, S. (2016). A dataset and evaluation metrics for abstractive compression of sentences and short paragraphs. In EMNLP.
- Tsai, S. C., Luo, J., Jiang, G., and Yeh, W. C. (2023). Adaptive fully sequential selection procedures with linear and nonlinear control variates. IIEE Transactions, 55(6):561–573.
- Van der Vaart, A. W. (2000). Asymptotic statistics, volume 3. Cambridge university press.
- Wang, T. and Hong, L. J. (2023). Large-scale inventory optimization: A recurrent neural networks-inspired simulation approach. INFORMS Journal on Computing, 35(1):196–215.
- Wang, W. and Chen, X. (2018). An adaptive two-stage dual metamodeling approach for stochastic simulation experiments. IIEE Transactions, 50(9):820–836.
- Wang, X., Hong, L. J., Jiang, Z., and Shen, H. (2023). Gaussian process-based random search for continuous optimization via simulation. Operations Research.
- Williams, R. J. (1992). Simple statistical gradient-following algorithms for connectionist reinforcement learning. Machine learning, 8:229–256.
- Wu, D., Wang, Y., and Zhou, E. (2022). Data-driven ranking and selection under input uncertainty. Operations Research.
- Wu, D., Zhu, H., and Zhou, E. (2018). A Bayesian risk approach to data-driven stochastic optimization: Formulations and asymptotics. SIAM Journal on Optimization, 28(2):1588–1612.
- Xie, W., Nelson, B. L., and Barton, R. R. (2014). A Bayesian framework for quantifying uncertainty in stochastic simulation. Operations Research, 62(6):1439–1452.
- Xie, W., Yi, Y., and Zheng, H. (2020). Global-local metamodel-assisted stochastic programming via simulation. ACM Transactions on Modeling and Computer Simulation (TOMACS), 31(1):1–34.
- Zamfirescu-Pereira, J., Wong, R. Y., Hartmann, B., and Yang, Q. (2023). Why johnny can’t prompt: how non-ai experts try (and fail) to design llm prompts. In Proceedings of the 2023 CHI Conference on Human Factors in Computing Systems, pages 1–21.
- Zhou, D., Li, L., and Gu, Q. (2020). Neural contextual bandits with ucb-based exploration. In International Conference on Machine Learning, pages 11492–11502. PMLR.
- Zhu, Y. and Dong, J. (2021). On constructing confidence region for model parameters in stochastic gradient descent via batch means. In 2021 Winter Simulation Conference (WSC), pages 1–12. IEEE.

Appendix

8. Score Function

In this section, we describe the score functions that are used to compare the similarity between the generated texts and the baseline text. The score function $h(x, y)$ compares the distance between two texts x and y . By regarding the text y as the baseline, a higher value of h indicates a higher similarity between two texts and therefore a higher score for x . Here we provide two examples of methods to compare similarities between texts: 1) cosine similarity and 2) Word2Vec (Church 2017). For a detailed overview of methods used to compare texts, we refer to Chandrasekaran and Mago (2021).

Cosine Similarity

Cosine similarity is a measure used to gauge the cosine of the angle between two non-zero vectors in an inner product space. This metric is particularly useful in the field of text analysis for comparing the similarity between documents or text data. The detailed procedure involves these steps:

1. **Vector Representation of Text:** First, each text document is converted into a vector. Each dimension of this vector represents a unique term (word) from the text. If a term occurs in the text, its value in the vector is non-zero. Examples of the representation include:

- **Term Frequency (TF):** The most commonly used representation for the non-zero value is TF, which stands for the number of times a term appears in the text;

- **Term Frequency-Inverse Document Frequency (TF-IDF):** TF is adjusted by the inverse document frequency (IDF) to down-weight terms that appear frequently across the texts. The TF-IDF value increases proportionally to the number of times a word appears in the document but is offset by the frequency of the word in the corpus.

In this way, the two texts to be compared are transformed into vectors with the same dimensionality, say $\mathbf{A}, \mathbf{B} \in \mathbb{R}^n$.

2. **Cosine Similarity between Vectors:** After we attain the two vectors \mathbf{A} and \mathbf{B} , the similarity between the two vectors is represented by the cosine similarity between two vectors as

$$\cos(\theta) = \frac{\mathbf{A} \cdot \mathbf{B}}{\|\mathbf{A}\| \|\mathbf{B}\|} = \frac{\sum_{i=1}^n A_i \times B_i}{\sqrt{\sum_{i=1}^n A_i^2} \times \sqrt{\sum_{i=1}^n B_i^2}},$$

where A_i, B_i denote the i -th entry of \mathbf{A}, \mathbf{B} , $\mathbf{A} \cdot \mathbf{B}$ is the dot product of vectors \mathbf{A} and \mathbf{B} , and $\|\mathbf{A}\|$ and $\|\mathbf{B}\|$ are the Euclidean norms of the vectors.

Word2Vec

Word2Vec is a technique in natural language processing (NLP) used to learn word embeddings, which are vector representations of words. Unlike simpler bag-of-words models like TF or TF-IDF, Word2Vec captures much richer semantic and syntactic relationships between words. There are

two main architectures in Word2Vec: Continuous Bag of Words (CBOW) and Skip-Gram. CBOW aims to predict a target word from its context words (surrounding words), and it takes multiple context words as input and tries to predict the word that is most likely to appear in the center of these context words. Skip-Gram, on the other hand, aims to predict context words from a target word. It takes a single word as input and tries to predict its surrounding context words. Here is a general mathematical representation

1. **Input Layer:** Each word in the vocabulary is represented as a one-hot encoded vector. In a vocabulary of size V , each word is a V -dimensional vector with one element set to 1 and the rest set to 0.

2. **Hidden Layer:** The hidden layer is a fully connected layer with N neurons, where N is the dimensionality of the word embeddings to learn. This layer serves as a lookup table: the output is the N -dimensional word vector corresponding to the input word.

3. **Output Layer:**

- For CBOW, the output layer is a softmax layer with v neurons (one for each word in the vocabulary). It outputs a probability distribution over the vocabulary, representing the likelihood of each word being the target word.

- For Skip-Gram, the output layer predicts multiple context words. Each context word prediction is a separate softmax operation over the vocabulary.

4. **Training:**

- The model is trained using pairs of context words and target words derived from sentences in the training corpus.

- The training objective is to maximize the probability of the correct target word (in CBOW) or context words (in Skip-Gram) given the input words, using a loss function like cross-entropy.

5. **Word Embeddings:** After training, the weights of the hidden layer become the word embeddings. Each row in the weight matrix corresponds to the vector representation of a particular word in the vocabulary.

After this procedure, Word2Vec then provides a numerical representation of the texts in the form of vectors. The distance defined on the vector space can be used to calculate the similarity between texts, and the selection of the vectors' distance is flexible, and can depend on the application.

9. Text Autoencoder

In this section, we provide details of the text autoencoder (Li et al. 2015, Kim et al. 2021), which is used in our framework to find the latent vectors of the human-readable prompts as in Section 3.1. To begin with, we first introduce the notion of “token”.

DEFINITION 1 (TOKEN). In the context of text processing and natural language processing (NLP), a “token” generally refers to an individual piece of a larger whole, usually a word, but it can also include punctuation marks, numbers, or other elements depending on the granularity of the tokenization process. In general, tokenization breaks down text into smaller parts (tokens). For example, the sentence “Prompts are helpful” can be tokenized into the tokens “Prompts,” “are,” and “helpful.”

By decomposing the input text into a series of tokens $x = \{x_1, x_2, \dots, x_n\}$, where x denotes the input text and x_i denotes the i -th token, the text autoencoder then transforms each token to a numerical vector (called as embedding), say e_i . Transforming a token x_i to an embedding involves mapping the token to an integer identification (ID) and then using this ID to look up a corresponding dense vector in an embedding matrix. This matrix is part of the model and is adjusted during training to capture semantic relationships between words. Here is a more detailed procedure:

1. **Token Representation:** Each unique token in the vocabulary is assigned a unique integer ID. For example, in a simple case, we have a vocabulary where “cat” is 1, “dog” is 2, etc. The token is then represented by its ID.

2. **Embedding Layer:** An embedding layer is essentially a lookup table that maps integer ID’s to high-dimensional vectors. This table is represented as a matrix E in general, where each row denotes a vector representation of a token in the vocabulary. If the embedding size is d and the vocabulary size is V , then $E \in \mathbb{R}^{V \times d}$, where each row $E_j \in \mathbb{R}^d$ denotes the embedding of the token with ID j .

3. **Lookup Process:** To find the embedding e_i of the token x_i , the model looks up the row in E that is identical to the integer ID of x_i . That is, if x_i is represented by the integer ID k , then the associated embedding is $e_i = E_k$, the k -th row of E .

4. **Learning:** Before learning from the data, the embeddings contained in E are usually initialized randomly. During the learning procedure (which we will describe later), these embeddings are adjusted through backpropagation based on the specific task the model is learning (e.g., classification, translation). The goal is to learn embeddings where similar or related words have similar embeddings. For example, in an effective text autoencoder model, the tokens “rabbit” and “bunny” will have different but similar embeddings, and the similarity is indicated by the distance between their numerical embeddings.

After transforming the tokens into embeddings, the input text is then represented by a sequence of numerical vectors $e = (e_1, e_2, \dots, e_n)$, where $e_n \in \mathbb{R}^d$ denotes the embedding of the n -th token in the input. In this way, the text input is then transformed into inputs that can be fed into a general autoencoder, which consists of two components: an encoder model and a decoder model. Both the

encoder model and the decoder model refer to the functionality and are not restricted to specific types of models. The selection of encoders and decoders depends on the forms of the input/output of the autoencoder model. Common selections include the recurrent neural network (RNN), the convolutional neural network (CNN), and the transformer. In some scenarios (specifically in NLP), both the inputs and output are sequences of embeddings that represent the texts and therefore are in the form of matrices. Here we generally denote them as vectors. Specifically, the encoder model transforms the input to a vector (named the latent vector) with a dimension lower than the input, and then the decoder model transforms the latent vector to a higher-dimensional vector. Mathematically, this procedure is represented by

$$X = f_{enc}(e)$$

and

$$y = f_{dec}(X),$$

where e is the input to the autoencoder, X denotes the latent vector, and y represents of the output of the autoencoder.

In the context of the text autoencoder, the output y , in the form of a numerical vector, is further transformed to text form $\text{text}(y)$ through a reverse process of the embedding process described above. In this way, for each input text x , the output of the text autoencoder is represented by $\text{text}(y(x))$ through the embedding process, the autoencoder model, and the reverse process of the embedding process. Given the structure of a text autoencoder, the learning process involves learning the parameters both contained in the embedding matrix and those in the encoder/decoder. Specifically, the learning procedure aims to choose the parameters that minimize

$$\sum_i \text{Loss}(\text{text}(y(x_i)), \tilde{y}_i),$$

where Loss is a selected loss function, (x_i, \tilde{y}_i) represents a pair of training data that contains the input x_i and the associated label \tilde{y}_i , which are both in text form. In addition, for the task of text reconstruction, $\tilde{y}_i = x_i$. That is, the text autoencoder is trained to generate the input text itself. In addition, we note that training an effective text autoencoder requires a large amount of data and computational resources. However, in our framework, we only have a set of example prompts. Therefore, we employ a pre-trained text autoencoder (Montero et al. 2021) and fine-tune it with the set of example prompts. After training, the latent vector then provides a numerical representation of each human-readable prompt.

10. Sampling Procedures

In the sequential evaluation step of our proposed framework, a Bayesian parametric model is used to approximate the mean score of the soft prompt as in Section 4.2.1. Given the historical observations of the score \mathcal{S}_t , the posterior distribution of the unknown parameters is represented by $p(\mathbf{W} | \mathcal{S}_t)$. When the posterior distribution does not adopt an explicit form, sampling algorithms are then required to generate samples $\{\widehat{\mathbf{W}}_1, \widehat{\mathbf{W}}_2, \dots, \widehat{\mathbf{W}}_K\}$ from the posterior distribution $p(\mathbf{W} | \mathcal{S}_t)$. Specifically, we select 1) the Hamilton Monte Carlo (HMC) algorithm and 2) variational inference (VI) as representatives.

11. Hamilton Monte Carlo

Here we describe the Hamilton Monte Carlo (HMC) algorithm (Girolami and Calderhead 2011), starting with the definition of its Hamiltonian.

DEFINITION 2 (HAMILTONIAN). The Hamiltonian $H(\mathbf{W}, \mathbf{m})$ of an HMC algorithm is defined as

$$H(\mathbf{W}, \mathbf{m}) = U(\mathbf{W}) + K(\mathbf{m}).$$

Here $U(\mathbf{W}) = -\log p(\mathcal{S}_t | \mathbf{W}) - \log(\pi(\mathbf{W}))$ is called *potential energy*, and $K(\mathbf{m}) = \frac{1}{2}\mathbf{m}^\top \mathbf{M}^{-1}\mathbf{m}$ is called *kinetic energy*, where $\mathbf{m} \in \mathbb{R}^d$ is the momentum vector and \mathbf{M} is a pre-specified mass matrix that is a positive definite and diagonal matrix. In general, \mathbf{M} is selected as an identity matrix if there is no prior knowledge.

The procedure of HMC is summarized as follows: 1. In each iteration, HMC samples a new momentum from a normal distribution, then enters a loop where it performs leapfrog steps to propose a new state in the parameter space. This involves making half a step in updating the momentum, a full step updating the parameters, and then another half step updating the momentum. 2. After leapfrogging, it computes a Metropolis acceptance probability to decide whether to accept or reject the new state. If accepted, the algorithm updates the parameters to the new state; if rejected, it retains the old state. This procedure leverages both the current position and momentum to explore the target distribution efficiently, leading to faster convergence compared to many other MCMC methods. The detailed procedure is presented in **Algorithm 3**.

12. Variational Inference

In this section, we provide the procedure of variational inference (VI) that is used to approximate an unknown probability; see also Blei et al. (2017). Here we specifically focus on approximating the posterior distribution $p(\mathbf{W} | \mathcal{S}_t)$, where \mathbf{W} denotes the unknown parameter and \mathcal{S}_t is the set of the observed data. VI aims to find an easy-to-simulate distribution family with an explicit form, say $q(\mathbf{W}; \boldsymbol{\lambda})$, $\boldsymbol{\lambda} \in \boldsymbol{\Lambda}$, and this distribution is used to approximate the posterior distribution $p(\mathbf{W} | \mathcal{S}_t)$.

Algorithm 3 Hamiltonian Monte Carlo algorithm for generating samples from $p(\mathbf{W} \mid \mathcal{S}_t)$

Input: The Hamiltonian $H(\mathbf{W}, \mathbf{m})$ regarding \mathbf{W} and \mathbf{m} ; initial parameters \mathbf{W}_0 , a positive definite and diagonal mass matrix \mathbf{M} , the number of required samples for the posterior distribution K , the number of samples to be discarded in the burn-in stage K' , a step size ϵ , and the number of iterations of a leapfrog step L .

Output: The samples from the posterior distribution $\{\widehat{\mathbf{W}}_1, \dots, \widehat{\mathbf{W}}_K\}$.

- 1: Let $k = 0$.
- 2: **while** $k < K' + K$ **do**
- 3: Sample momentum $\mathbf{m}_k \sim \mathcal{N}(\mathbf{0}, \mathbf{M})$.
- 4: Set $\mathbf{W}^{(k+1)} = \mathbf{W}_k$ and $\mathbf{m}^{(k+1)} = \mathbf{m}_k$.
- 5: **for** $l = 1$ to L **do**
- 6: Update $\mathbf{m}^{(k+1)} = \mathbf{m}^{(k+1)} - \frac{\epsilon}{2} \nabla_{\mathbf{W}} U(\mathbf{W}^{(k+1)})$.
- 7: Update $\mathbf{W}^{(k+1)} = \mathbf{W}^{(k+1)} + \epsilon \mathbf{m}^{(k+1)}$.
- 8: Update $\mathbf{m}^{(k+1)} = \mathbf{m}^{(k+1)} - \frac{\epsilon}{2} \nabla_{\mathbf{W}} U(\mathbf{W}^{(k+1)})$.
- 9: **end for**
- 10: Compute Metropolis acceptance probability $\alpha_c = \min\left(1, \frac{\exp(-H(\mathbf{W}^{(k+1)}, \mathbf{m}^{(k+1)}))}{\exp(-H(\mathbf{W}_k, \mathbf{m}_k))}\right)$.
- 11: Sample $u \sim \text{Uniform}(0, 1)$
- 12: **if** $u < \alpha_c$ **then**
- 13: Accept the new state: $(\mathbf{W}_{k+1}, \mathbf{m}_{k+1}) = (\mathbf{W}^{(k+1)}, \mathbf{m}^{(k+1)})$ and let $k = k + 1$.
- 14: **if** $k > K'$ **then**
- 15: Let $\widehat{\mathbf{W}}_{k-K'} = \mathbf{W}_k$.
- 16: **end if**
- 17: **end if**
- 18: **end while**
- 19: **return** The samples from the posterior distribution $\{\widehat{\mathbf{W}}_1, \dots, \widehat{\mathbf{W}}_K\}$.

The approximation is facilitated by optimizing the parameter $\boldsymbol{\lambda} \in \boldsymbol{\Lambda}$ to minimize the distance (e.g., Kullback–Leibler divergence) between $q(\mathbf{W}; \boldsymbol{\lambda})$ and $p(\mathbf{W} \mid \mathcal{S}_t)$. After determining the variational distribution $q(\mathbf{W}; \boldsymbol{\lambda}^*)$, samples of $\widehat{\mathbf{W}} \sim q(\mathbf{W}; \boldsymbol{\lambda}^*)$ are efficiently generated for inference.

Furthermore, the Kullback-Leibler divergence between the variational distribution $q(\mathbf{w} \mid \boldsymbol{\lambda})$ and the posterior distribution $p(\mathbf{W} \mid \mathcal{S}_t)$ is challenging to directly optimize in some scenarios. Instead, an equivalent procedure is maximizing the Evidence Lower Bound (ELBO):

$$\text{ELBO}(\boldsymbol{\lambda}) = \mathbb{E}_{q(\mathbf{w}; \boldsymbol{\lambda})} [\log p(\mathcal{S}_t, \mathbf{W}) - \log q(\mathbf{W}; \boldsymbol{\lambda})].$$

The maximization of ELBO is largely supported by the stochastic gradient ascent by generating samples from the variational distribution $q(\mathbf{W}; \boldsymbol{\lambda})$. This can be accomplished efficiently since the variational distribution is selected to be easy to simulate. After deciding an optimal $\boldsymbol{\lambda}^*$ that maximizes ELBO, samples $\{\widehat{\mathbf{W}}_1, \widehat{\mathbf{W}}_2, \dots, \widehat{\mathbf{W}}_K\}$ are then generated from $q(\mathbf{W}; \boldsymbol{\lambda}^*)$. We summarize the procedure in **Algorithm 4**.

Algorithm 4 Variational inference for approximating posterior distribution $p(\mathbf{W}|\mathcal{S}_t)$

Input: A family of variational distributions $q(\mathbf{W}|\boldsymbol{\lambda})$, $\boldsymbol{\lambda} \in \boldsymbol{\Lambda}$, a selected stochastic gradient ascent algorithm with N iterations, and a learning rate η .

Output: The approximate posterior distribution $q(\mathbf{W}|\boldsymbol{\lambda}^*)$.

Initialize variational parameters $\boldsymbol{\lambda}$.

for $i \in \{1, 2, \dots, N\}$ **do**

Compute the gradient $\nabla_{\boldsymbol{\lambda}} \text{ELBO}(\boldsymbol{\lambda})$.

Update the variational parameters: $\boldsymbol{\lambda} \leftarrow \boldsymbol{\lambda} + \eta \nabla_{\boldsymbol{\lambda}} \text{ELBO}(\boldsymbol{\lambda})$.

end for

Set $\boldsymbol{\lambda}^* = \boldsymbol{\lambda}$.

return The approximate posterior distribution $q(\mathbf{W}|\boldsymbol{\lambda}^*)$.

13. Proof

In this section, we present the proof of theoretical results in the main text.

13.1. Proof of Theorem 1

To prove the consistency of **Algorithm 1**, we first assume that not all the soft prompts will be evaluated an infinite number of times when the total budget $T \rightarrow \infty$. Since the number of soft prompts is finite, as $T \rightarrow \infty$, there will always be some soft prompts that are evaluated an infinite number of times, and we denote by

$$\mathcal{Z}_{\infty} = \left\{ z_n \mid \lim_{T \rightarrow \infty} r_n(T) = \infty \right\},$$

the set of such soft prompts. Recall that the posterior distribution of the unknown parameters is

$$p(\mathbf{W} | \mathcal{S}_t) = \frac{p(\mathcal{S}_t | \mathbf{W}) \pi(\mathbf{W})}{p(\mathcal{S}_t)} \propto p(\mathcal{S}_t | \mathbf{W}) \pi(\mathbf{W}),$$

where

$$p(\mathcal{S}_t | \mathbf{W}) = \prod_{n=1}^N \prod_{m=1}^{r_n(t)} \frac{1}{\sqrt{2\pi\sigma_n^2}} \exp\left(-\frac{(\widehat{v}_{n,m} - \mathbf{f}(z_n; \mathbf{W}))^2}{2\sigma_n^2}\right)$$

is the likelihood of the observed scores and \mathcal{S}_t denotes the set of the observed scores up to time t .

We note that, for any selected $z_m \in \mathcal{Z}$, $\mathbf{f}(z_m; \widehat{\mathbf{W}})$, $\widehat{\mathbf{W}} \sim p(\mathbf{W} | \mathcal{S}_t)$ serves as the approximation of the mean score $v(z_m)$, and the posterior variance

$$\lim_{t \rightarrow \infty} \text{Var} \left[\mathbf{f}(z_m; \widehat{\mathbf{W}}) | \mathcal{S}_t \right] \stackrel{w.p.1}{=} 0. \quad (17)$$

To see this, we first consider a simple case where we are forced to evaluate only one fixed prompt z_1 . In this way, it will be evaluated an infinite number of times and we observe $\mathcal{S}_t^{(1)} = \{\widehat{v}_{1,1}, \widehat{v}_{1,2}, \dots, \widehat{v}_{1,t}\}$. Since $\forall z_n \in \mathcal{Z}$, $\mathbf{f}(z_n; \mathbf{W}) \neq \mathbf{f}(z_n; \mathbf{W}')$ when $\mathbf{W} \neq \mathbf{W}'$, and $\widehat{v}_{1,m} \stackrel{i.i.d.}{\sim} \mathcal{N}(\mathbf{f}(z_1; \mathbf{W}), \sigma_1^2)$, by Doob's consistency theorem (Van der Vaart 2000, Miller 2018), for any integrable function g , we have

$$\lim_{t \rightarrow \infty} \mathbb{E} \left[g(\widehat{\mathbf{W}}) | \mathcal{S}_t^{(1)} \right] \stackrel{w.p.1}{=} g(\mathbf{W}).$$

Thus, we have

$$\lim_{t \rightarrow \infty} \text{Var} \left[\mathbf{f}(z_1; \widehat{\mathbf{W}}) | \mathcal{S}_t^{(1)} \right] = \lim_{t \rightarrow \infty} \mathbb{E} \left[\mathbf{f}^2(z_1; \widehat{\mathbf{W}}) | \mathcal{S}_t^{(1)} \right] - \lim_{t \rightarrow \infty} \left[\mathbb{E} \left[\mathbf{f}(z_1; \widehat{\mathbf{W}}) | \mathcal{S}_t^{(1)} \right] \right]^2 \stackrel{w.p.1}{=} 0 \quad (18)$$

where

$$p(\mathbf{W} | \mathcal{S}_t^{(1)}) = \frac{p(\mathcal{S}_t^{(1)} | \mathbf{W}) \pi(\mathbf{W})}{\int p(\mathcal{S}_t^{(1)} | \mathbf{W}) \pi(\mathbf{W}) d\mathbf{W}}.$$

Recall that soft prompts are classified into two categories, \mathcal{Z}_∞ and $\mathcal{Z} \setminus \mathcal{Z}_\infty$. Compared with the special scenario in (18) where the observations are i.i.d., the general scenario we want to show, as in (17), has two main differences: 1) there are soft prompts that only provide a finite number of observations and 2) there might be multiple soft prompts that are evaluated an infinite number of times. Thus, to prove the statement in (17), we must show that these two differences will not change the convergence. Since the number of soft prompts is finite, without loss of generality, we consider two simplified scenarios. In the first scenario, there are two soft prompts to be evaluated, say z_1 and z_2 , and z_1 will be evaluated an infinite number of times and z_2 will only be evaluated $n_s < \infty$ times. In this way, we consider the likelihood function when t is sufficiently large is

$$p(\mathcal{S}_t^{(1)}, \mathcal{S}_t^{(2)} | \mathbf{W}) = \left(\prod_{m=1}^{t-n_s} p(\widehat{v}_{1,m} | \mathbf{W}) \right) \left(\prod_{m=1}^{n_s} p(\widehat{v}_{2,m} | \mathbf{W}) \right).$$

The posterior distribution is then

$$\begin{aligned} p(\mathbf{W} | \mathcal{S}_t^{(1)}, \mathcal{S}_t^{(2)}) &= \frac{\left(\prod_{m=1}^{t-n_s} p(\widehat{v}_{1,m} | \mathbf{W}) \right) \left(\prod_{m=1}^{n_s} p(\widehat{v}_{2,m} | \mathbf{W}) \right) \pi(\mathbf{W})}{\int \left(\prod_{m=1}^{t-n_s} p(\widehat{v}_{1,m} | \mathbf{W}) \right) \left(\prod_{m=1}^{n_s} p(\widehat{v}_{2,m} | \mathbf{W}) \right) \pi(\mathbf{W}) d\mathbf{W}} \\ &= \frac{\left(\prod_{m=1}^{t-n_s} p(\widehat{v}_{1,m} | \mathbf{W}) \right) \pi'(\mathbf{W})}{\int \left(\prod_{m=1}^{t-n_s} p(\widehat{v}_{1,m} | \mathbf{W}) \right) \pi'(\mathbf{W}) d\mathbf{W}} \end{aligned}$$

Here $\pi'(\mathbf{W}) = (\prod_{m=1}^{n_s} p(\widehat{v}_{2,m} | \mathbf{W})) \pi(\mathbf{W})$ is fixed as $t \rightarrow \infty$ since z_2 will only be evaluated $n_s < \infty$ times. In other words, the prior distribution $\pi(\mathbf{W})$ is rescaled by $\mathcal{S}_t^{(2)}$. Thus, by applying Doob's consistency theorem and letting $t \rightarrow \infty$, we attain an analogous result to (18). Thus, the observed scores for the soft prompts in $\mathcal{Z} \setminus \mathcal{Z}_\infty$ will not influence the convergence described in (17).

Next, we see that for different soft prompts in $z_n \in \mathcal{Z}$, although the increasing rates $r_n(t)$ might differ as $t \rightarrow \infty$, the convergence remains. Without loss of generality, we consider two soft prompts that are both evaluated an infinite number of times, say z_1 and z_3 . We then denote two filtrations as

$$\begin{aligned} \mathfrak{F}_m &= \sigma \{(\widehat{v}_{1,1}, \widehat{v}_{3,1}), (\widehat{v}_{1,2}, \widehat{v}_{3,2}), \dots, (\widehat{v}_{1,m}, \widehat{v}_{3,m})\}, \\ \mathfrak{G}_{m,k} &= \sigma \{\widehat{v}_{1,1}, \dots, \widehat{v}_{1,m}, \widehat{v}_{3,1}, \dots, \widehat{v}_{3,k}\}. \end{aligned}$$

Thus, we have $\mathfrak{G}_{m,k} \subseteq \mathfrak{F}_{m \wedge k}$, where $m \wedge k = \max\{m, k\}$. In addition, we note that

$$\lim_{m \rightarrow \infty} \text{Var} \left[\mathbf{f} \left(z_n; \widehat{\mathbf{W}} \right) \mid \mathfrak{F}_m \right] \stackrel{w.p.1}{=} 0, \quad \forall z_n \in \mathcal{Z}$$

by regarding $(\widehat{v}_{1,m}, \widehat{v}_{3,m})$ as i.i.d. samples from a joint distribution. Then we have

$$\begin{aligned} \left| \mathbb{E} \left[g \left(\widehat{\mathbf{W}} \right) \mid \mathfrak{G}_{m,k} \right] - g(\mathbf{W}) \right| &= \left| \mathbb{E} \left[\mathbb{E} \left[g \left(\widehat{\mathbf{W}} \right) \mid \mathfrak{F}_{m \wedge k} \right] - g(\mathbf{W}) \mid \mathfrak{G}_{m,k} \right] \right| \\ &\leq \mathbb{E} \left[\left| \mathbb{E} \left[g \left(\widehat{\mathbf{W}} \right) \mid \mathfrak{F}_{m \wedge k} \right] - g(\mathbf{W}) \right| \mid \mathfrak{G}_{m,k} \right] \end{aligned} \quad (19)$$

for an integrable g . Note that $\forall z_n \in \mathcal{Z}$, both $\mathbf{f}(z_n; \mathbf{W})$ and $\mathbf{f}^2(z_n; \mathbf{W})$ are integrable. By replacing g in (19) with $\mathbf{f}(z_n; \mathbf{W})$ and $\mathbf{f}^2(z_n; \mathbf{W})$ respectively, we then have

$$\lim_{m,k \rightarrow \infty} \text{Var} [\mathbf{f}(z_n; \mathbf{W}) \mid \mathfrak{G}_{m,k}] \stackrel{w.p.1}{=} 0$$

from the dominated convergence theorem, giving us (17). That is, for every soft prompt $z_n \in \mathcal{Z}$, the posterior variance of $\mathbf{f}(z_n; \widehat{\mathbf{W}})$ shrinks to zero as $t \rightarrow \infty$.

On the other hand, maximizing the acquisition function M-UCB is equivalent to maximizing a rescaled M-UCB

$$\alpha'_t(z_n) = \frac{\mu_t(z_n)}{\beta_t} + \sigma_t(z_n) + \gamma(r_n(t)).$$

As $\lim_{t \rightarrow \infty} \beta_t = \infty$, and $\lim_{r_n(t) \rightarrow \infty} \gamma(r_n(t)) = 0$, we have

$$\lim_{t \rightarrow \infty} \alpha'_t(z_n) \begin{cases} = 0, & \forall z_n \in \mathcal{Z}_\infty \\ > 0, & \forall z_n \in \mathcal{Z} \setminus \mathcal{Z}_\infty \end{cases}. \quad (20)$$

Since the soft prompt selected in each iteration is the soft prompt that maximizes the (rescaled) acquisition function, which contradicts (20), the assumption that $\mathcal{Z}_\infty \subsetneq \mathcal{Z}$ is violated. Thus, every soft prompt will be evaluated an infinite number of times with probability one as the total budget T approaches infinity.

Because the evaluation uncertainty is Gaussian noise and is independently and identically distributed, the strong law of large numbers holds (Van der Vaart 2000), and for any $z_m \notin \arg \max_{z_n} v(z_n)$, there will be a discrepancy, say δ . Thus, when T is sufficiently large, we have

$$\bar{v}(z_m) < v(z_m) + \frac{\delta}{2} < v(z^*) - \frac{\delta}{2} < \bar{v}(z^*)$$

with probability one. In other words, when $T \rightarrow \infty$, the soft prompts that are not optimal will not be selected.

13.2. Proof of Theorem 2

In this section, we prove the consistency of the probabilistic reparametrization of the acquisition function and propositions in Section 4.2.2.

Regarding Proposition 1, because

$$\mathbb{E}[\mathbf{f}^2(z_n; \mathbf{W}) \mid \mathcal{S}_t] < \infty \quad \forall z_n \in \mathcal{Z},$$

we have

$$\lim_{K \rightarrow \infty} \hat{\alpha}_t(z_n) \stackrel{w.p.1}{=} \alpha_t(z_n)$$

from the strong law of large numbers (Van der Vaart 2000). Furthermore, since there are only a finite number of z_n 's in \mathcal{Z} , this convergence is uniform. That is,

$$\lim_{K \rightarrow \infty} \left\{ \delta_K \doteq \max_{z_n \in \mathcal{Z}} \{ \hat{\alpha}_t(z_n) - \alpha_t(z_n) \} \right\} \stackrel{w.p.1}{=} 0.$$

Thus, we prove Proposition 1 because

$$|\hat{\alpha}_t(z^*) - \alpha_t(z^{(t+1)})| \leq \delta_K.$$

Regarding Theorem 2, we consider a mapping

$$\varphi: [0, 1]^N \rightarrow \mathcal{P}_{\mathcal{Z}},$$

with

$$p_{\varphi(\theta)}(\{z_i\}) = \frac{\theta^{(i)}}{\sum_{j=1}^N \theta^{(j)}},$$

which maps $\theta \in \Theta = [0, 1]^N$ to a discrete probability distribution $\mathcal{P}_{\mathcal{Z}}$ defined on $\mathcal{Z} = \{z_1, z_2, \dots, z_N\}$. Here $\theta^{(i)}$ represents the i -th entry of θ . We note that this function is continuous in θ by regarding $(\mathcal{P}_{\mathcal{Z}}, \|\cdot\|)$ as a metric space with any norm $\|\cdot\|$ defined on an N -dimensional vector space.

Furthermore, for any $\theta^* \in \mathcal{J}_t^* = \{\theta \mid \theta \in \arg \max_{\theta \in \Theta} \hat{\alpha}_t(\theta)\}$ and $z^* \in \text{support}(p(z_n; \theta^*))$, we have $z^* \in \mathcal{H}_t^*$. To prove this, we assume that there exists $z' \in \text{support}(p(z_n; \theta^*))$ and $z' \notin \mathcal{H}_t^*$. Thus,

$$p_{\varphi(\theta^*)}(\{z'\}) > 0.$$

We consider a probability measure

$$p'(\{z\}) = \begin{cases} 0 & \text{if } z = z' \\ p_{\varphi(\theta^*)}(\{z^*\}) + p_{\varphi(\theta^*)}(\{z'\}) & \text{if } z = z^* \\ p_{\varphi(\theta^*)}(\{z\}) & \text{otherwise.} \end{cases}$$

In this way, we have

$$\mathbb{E}_{p'(\{z\})}[\alpha_t(z_n)] = \alpha_t(z^*) + p_{\varphi(\theta^*)}(\{z'\}) (\alpha_t(z^*) - \alpha_t(z')) > \alpha_t(z^*).$$

On the other hand, since $\varphi(\theta)$ is continuous, there will be a $\theta' \in \Theta$ such that $\varphi(\theta') = p'$, which contradicts the assumption that $\theta^* \in \mathcal{J}_t^*$. Therefore, we have $z' \in \mathcal{H}_t^*$ and

$$\hat{\mathcal{H}}_t^* \subseteq \mathcal{H}_t^*. \quad (21)$$

Next, we prove that if $z^* \in \mathcal{H}_t^*$, then

$$\alpha_t(z^*) = \max_{\theta \in \Theta} \tilde{\alpha}_t(\theta). \quad (22)$$

To see this, for any $z^* \in \mathcal{H}_t^*$, we set θ^* be the parameters such that $p(z^*; \theta^*) = 1$. In this way, to prove (22), we assume that there exists θ' such that $\tilde{\alpha}_t(\theta') > \tilde{\alpha}_t(\theta^*)$. On the other hand, since $z^* \in \arg \max_{z_n} \alpha_t(z_n)$, no convex combinations (expected values) of α_t can be larger. Thus, there is contradiction and (22) holds. Therefore,

$$\mathcal{H}_t^* \subseteq \hat{\mathcal{H}}_t^*.$$

By taking (21) into consideration, we have that

$$\hat{\mathcal{H}}_t^* = \mathcal{H}_t^*.$$

Furthermore, we note that φ is differentiable in θ for any given z_n . Thus, PR-M-UCB is a finite combination of differentiable $p(z_n; \theta) \alpha_t(z_n)$'s, and therefore is also differentiable. Moreover, because

$$\nabla_{\theta} \log p(z_n | \theta) = \frac{\nabla_{\theta} p(z | \theta)}{p(z_n | \theta)},$$

we have

$$\begin{aligned} \nabla_{\theta} \mathbb{E}_{p(z_n; \theta)}[\alpha_t(z_n)] &= \sum_{n=1}^N \alpha_t(z_n) \nabla_{\theta} p(z_n; \theta) \\ &= \sum_{n=1}^N \alpha_t(z_n) \nabla_{\theta} \log p(z_n | \theta) p(z_n; \theta) \\ &= \mathbb{E}_{p(z_n; \theta)}[\alpha_t(z_n) \nabla_{\theta} \log p(z_n | \theta)]. \end{aligned}$$

Thus, we prove Proposition 3. The unbiased estimator $\widehat{\nabla}_\theta \tilde{\alpha}_t(\theta) \doteq \frac{1}{I} \sum_{i=1}^I \alpha_t(\tilde{z}_i) \nabla_\theta \log(p(\tilde{z}_i; \theta))$ is also known as REINFORCE (Williams 1992) and the likelihood ratio estimator (Glynn and Olvera-Cravioto 2019).

In addition, we note that the maximization of PR-M-UCB is reformulated as a linear programming problem when we impose the constraint $\sum_{i=1}^N \theta^{(i)} = 1$. On the other hand, the coefficients $(\alpha_t(z_1), \alpha_t(z_2), \dots, \alpha_t(z_N))$ in the objective function are unknown and require estimation, which is time-consuming if N is large. Therefore, we employ stochastic gradient ascent to optimize PR-M-UCB. We refer to Louveaux and Schultz (2003) for detailed discussions on stochastic linear programming.

13.3. Proof of Theorem 3

In this section, we provide the upper bound of the cumulative uncertainty of the PSK predictor $U_I = \sum_{i=1}^I \widehat{\sigma}^2(\tilde{X}_i)$, where $\widehat{\sigma}^2(\cdot)$ is the prediction uncertainty of the PSK predictor. First, we have

$$\widehat{\sigma}^2(X) \leq \sup_{X \in \tilde{\mathcal{X}}} \left\| \tilde{A}^*(X) \right\|^2 \leq A_M$$

for some constant $A_M > 0$. Then, since $\frac{s}{\log(1+s)}$ is a non-decreasing function with $s > 0$, we have

$$\widehat{\sigma}^2(\tilde{X}_i) \leq \frac{A_M}{\log(1 + A_M \underline{\sigma}_\epsilon^{-2})} \log\left(1 + \underline{\sigma}_\epsilon^{-2} \widehat{\sigma}^2(\tilde{X}_i)\right) \quad (23)$$

for each additional evaluation $\tilde{X}_i \in \mathcal{R}$. Here $\underline{\sigma}_\epsilon^{-2} \widehat{\sigma}^2 = \inf_{X \in \tilde{\mathcal{X}}} \sigma_\epsilon^2(X)$.

We then employ the information gain (Cover 1999) of the Gaussian process, which is

$$\mathcal{I}(\widehat{V}_j; V_j) = H(\widehat{V}_j) - H(\widehat{V}_j | V_j),$$

where $\widehat{V}_j = (\widehat{v}(\tilde{X}_1), \dots, \widehat{v}(\tilde{X}_j))^\top$ is the vector of the observations, and $V_j = (v(\tilde{X}_1), \dots, v(\tilde{X}_j))^\top$ denotes the mean score vector. Also, $H(\widehat{V}_j)$ is the entropy of \widehat{V}_j and $H(\widehat{V}_j | V_j)$ denotes the conditional entropy of \widehat{V}_j on V_j . Note that, for a Gaussian random vector $\xi \sim \mathcal{N}(\boldsymbol{\mu}, \boldsymbol{\Sigma})$, $H(\xi) = \frac{1}{2} \log |2\pi e \boldsymbol{\Sigma}|$, where e is Euler's number. Thus

$$\begin{aligned} H(\widehat{V}_j) &= H(\widehat{V}_{j-1}) + H(\widehat{v}(\tilde{X}_j) | \widehat{V}_{j-1}) \\ &= H(\widehat{V}_{j-1}) + \frac{1}{2} \log\left(2\pi e \left(\sigma_\epsilon^2(\tilde{X}_j) + \widehat{\sigma}^2(\tilde{X}_j)\right)\right) \\ &\geq H(\widehat{V}_{j-1}) + \frac{1}{2} \log\left(2\pi e \left(\underline{\sigma}_\epsilon^2 + \widehat{\sigma}^2(\tilde{X}_j)\right)\right). \end{aligned}$$

Since $\mathcal{I}(\widehat{V}_I; V_I) = H(\widehat{V}_I) - H(\widehat{V}_I | V_I)$, we then have

$$\mathcal{I}(\widehat{V}_I; V_I) \geq \frac{1}{2} \sum_{i=1}^I \log\left(1 + \underline{\sigma}_\epsilon^{-2} \widehat{\sigma}^2(\tilde{X}_i)\right).$$

Therefore, considering (23), the cumulative uncertainty is bounded by

$$U_I = \sum_{i=1}^I \widehat{\sigma}^2(\tilde{X}_i) \leq \frac{2A_M}{\log(1 + A_M \underline{\sigma}_\epsilon^{-2})} \mathcal{I}(\widehat{V}_I; V_I). \quad (24)$$

Next, we provide the upper bound of $\mathcal{I}(\widehat{V}_I; V_I)$. Specifically,

$$\begin{aligned} \mathcal{I}(\widehat{V}_I; V_I) &= H(\widehat{V}_I) - H(\widehat{V}_I | V_I) \\ &= \frac{1}{2} \log \left| 2\pi e \left(\mathbf{K}_I + \text{Diag} \left\{ \sigma_\epsilon^2(\tilde{X}_1), \sigma_\epsilon^2(\tilde{X}_2), \dots, \sigma_\epsilon^2(\tilde{X}_I) \right\} \right) \right| \\ &\quad - \frac{1}{2} \log \left| 2\pi e \cdot \text{Diag} \left\{ \sigma_\epsilon^2(\tilde{X}_1), \sigma_\epsilon^2(\tilde{X}_2), \dots, \sigma_\epsilon^2(\tilde{X}_I) \right\} \right| \\ &\leq \frac{1}{2} \log \left| \underline{\sigma}_\epsilon^{-2} \mathbf{K}_I + \overline{\sigma}_\epsilon^2 / \underline{\sigma}_\epsilon^2 \mathbf{I}_I \right|, \end{aligned} \quad (25)$$

where \mathbf{I}_I denotes the I -dimensional identity matrix, and \mathbf{K}_I denotes the kernel matrix

$$\begin{pmatrix} \tilde{A}^*(\tilde{X}_1)^\top \\ \vdots \\ \tilde{A}^*(\tilde{X}_I)^\top \end{pmatrix} \left(\tilde{A}^*(\tilde{X}_1), \dots, \tilde{A}^*(\tilde{X}_I) \right) \in \mathbb{R}^{I \times I}.$$

Denote $\mathbf{A}_I = \left(\tilde{A}^*(\tilde{X}_1), \dots, \tilde{A}^*(\tilde{X}_I) \right) \in \mathbb{R}^{D^* \times I}$. Thus $\mathbf{K}_I = \mathbf{A}_I^\top \mathbf{A}_I$. Note that,

$$\begin{aligned} \left| \overline{\sigma}_\epsilon^2 / \underline{\sigma}_\epsilon^2 \mathbf{I}_I + \underline{\sigma}_\epsilon^{-2} \mathbf{A}_I^\top \mathbf{A}_I \right| &= \left| \overline{\sigma}_\epsilon^2 / \underline{\sigma}_\epsilon^2 \mathbf{I}_{D^*} + \underline{\sigma}_\epsilon^{-2} \mathbf{A}_I \mathbf{A}_I^\top \right| \\ &\leq \prod_{d=1}^{D^*} \left(\overline{\sigma}_\epsilon^2 / \underline{\sigma}_\epsilon^2 + \underline{\sigma}_\epsilon^{-2} \mathbf{a}_{dd} \right), \end{aligned}$$

where \mathbf{a}_{dd} denotes the (d, d) -th entry of $\mathbf{A}_I \mathbf{A}_I^\top \in \mathbb{R}^{D^* \times D^*}$. Here the equality comes from that $\mathbf{A}_I^\top \mathbf{A}_I$ and $\mathbf{A}_I \mathbf{A}_I^\top$ have the same non-zero eigenvalues, and the inequality comes from the Hadamard inequality; see Garling (2007). Since the norm of $A^*(X)$ is bounded, the largest eigenvalue of $\mathbf{A}_I \mathbf{A}_I^\top$ is at most at order of I . Thus,

$$\log \left| \overline{\sigma}_\epsilon^2 / \underline{\sigma}_\epsilon^2 \mathbf{I}_I + \underline{\sigma}_\epsilon^{-2} \mathbf{A}_I^\top \mathbf{A}_I \right| = \mathcal{O}(D^* \log I),$$

which provides the upper bound of the cumulative uncertainty U_I considering both (24) and (25).

14. Surrogate Models

In this section, we provide details of the surrogate models used in our experiments to approximate the mean score function with respect to the soft prompt. Specifically, we consider surrogate models including 1) the Bayesian linear regression model, 2) the Gaussian process (GP) process model, 3) the Bayesian neural network (BNN) model, and 4) the variational autoencoder (VAE). In terms of GP and BNN, the descriptions are contained in Section 4.2.1 as examples. Here we focus on the Bayesian linear regression model and VAE.

14.1. Bayesian Linear Regression

Bayesian linear regression is a statistical method in which we use Bayes' Theorem to estimate the parameters of a linear regression model. In Bayesian linear regression, the model parameters are treated as random variables and a prior probability distribution is imposed on these parameters. This distribution is then updated by Bayes' Theorem with the observed data.

Specifically, the model is represented by

$$\hat{v}(z) = \mathbf{W}^\top z + \epsilon,$$

where $\hat{v}(z)$ is the predicted output, z is the input vector, \mathbf{W} is the vector of unknown weights or parameters, and ϵ is the noise term, typically assumed to be Gaussian with zero mean and variance σ^2 .

In Bayesian linear regression, rather than finding single point estimates of \mathbf{W} , we calculate the posterior distribution of \mathbf{W} given the data. This is done using Bayes' theorem:

$$P(\mathbf{W} | \mathbf{Z}, \mathbf{V}) = \frac{P(\mathbf{V} | \mathbf{Z}, \mathbf{W})\pi(\mathbf{W})}{P(\mathbf{V} | \mathbf{Z})}$$

where \mathbf{Z} is the matrix of input data, \mathbf{V} is the vector of output data, $\pi(\mathbf{W})$ is the prior distribution of \mathbf{W} , $P(\mathbf{V} | \mathbf{Z}, \mathbf{W})$ is the likelihood of observing \mathbf{V} given \mathbf{Z} and \mathbf{W} , and $P(\mathbf{V} | \mathbf{Z})$ is the marginal likelihood or evidence. Here we assume that the variance of the noise σ^2 is known. In this way, a common selected prior of the unknown parameters is the Gaussian distribution, that is, $P(\mathbf{W}) = \mathcal{N}(\mathbf{W} | \boldsymbol{\mu}_0, \boldsymbol{\Sigma}_0)$, where $\boldsymbol{\mu}_0, \boldsymbol{\Sigma}_0$ are user-specified. We refer to [Minka \(2000\)](#) for a more detailed description.

14.2. Variational Autoencoder

Recall that in Section 9, we describe the model of text autoencoder, in which tokens are first transformed to numerical representations and then fed into an autoencoder model. VAE, as a type of autoencoder model, is also composed of two components: 1) an encoder model and 2) a decoder model, and encoder/decoder models are largely neural networks, and depend on the applications. The difference between a regular autoencoder and VAE is that the input (numerical representation) is transformed into a latent vector in the latent space by the encoder of a regular autoencoder model. In the VAE model, each input, say z , fed into the encoder is then mapped to a distribution in the latent space, say $p(y | z, \mathbf{W}_{enc})$. Here y denotes the latent vectors that are random, z is the input to VAE and \mathbf{W}_{enc} denotes the unknown parameters in the encoder part. The latent vector, once generated, is then mapped by the coder model to the output of VAE. In this way, given a fixed input of z , VAE will generate different samples of latent vectors $\{y_1, y_2, \dots, y_K\}$ and then provide a set of outputs. This generative property allows VAEs to be powerful tools for both supervised and

unsupervised learning problems, particularly in tasks like image generation, anomaly detection, and feature extraction.

In a VAE model, the unknown parameters are implicitly contained in the encoder/decoder models. That is, if the encoder and the decoder are both selected to be neural networks, the unknown parameters of VAE are the weight parameters of the neural networks. As a Bayesian parametric model, the unknown parameters can be updated by the Bayes’ Theorem and the method of variational inference is widely employed to approximate the posterior distribution of the unknown parameters. On the other hand, when the encoder and decoder models are complex models (e.g., transformers), it is challenging to approximate the posterior distribution, even for the method of variational inference. Instead, an alternative method to train VAE is to minimize a combined loss function

$$\mathcal{L}_{\text{total}} = \mathcal{L}_{\text{regression}} + \beta \times \mathcal{L}_{KL},$$

where $\mathcal{L}_{\text{regression}}$ denotes the loss between the observed ground-truth data and the predicted output generated by VAE, and \mathcal{L}_{KL} quantifies the distance (Kullback–Leibler divergence) between the learned latent space representation and a predefined distribution (usually a standard normal distribution), providing a form of regularization. For more detailed discussions of VAE, we refer to [Kingma et al. \(2019\)](#).

15. Selected Prompts

In **Table 1**, we present the selected prompts using the algorithm M-UCB-r (described in Section 6.3) regarding all six tasks. The experimental setting is consistent with that in **Figure 8**.

Table 1 Selected prompts for six tasks using M-UCB-r.

Task	turbo-3.5	davinci-003
word sorting	Sort the following word list in alphabetic order.	Sort the words in alphabet order.
first letter	Return the first letter of the selected word.	Select the initial letter in the word.
counting objectives	Count the total number of mentioned products.	Estimate the total quantity for all products.
rhymes	Choose the word with the closest pronunciation.	Select the word with most similar pronunciation.
nums to verbal	Turn number list to word list.	Turn number list to word list.
largest animals	Choose the larger animal from the following animals.	Select the largest animals in size.